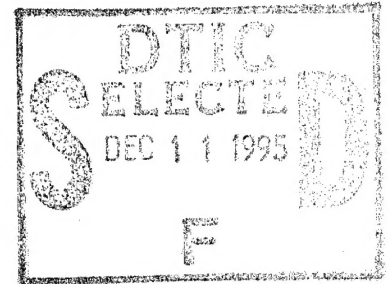


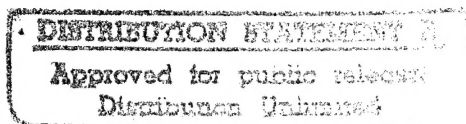
NASA Contractor Report 3106



# Analysis of Graphite/Polyimide Rail Shear Specimens Subjected to Mechanical and Thermal Loading

Terry A. Weisshaar and Ramon Garcia

GRANT NGR-47-004-129  
MARCH 1979



DEPARTMENT OF DEFENSE  
PLASTICS TECHNICAL EVALUATION CENTER  
ARRADCOM, DOVER, N. J. 07801

19951128 140

**NASA**

DTIC QUALITY INSPECTED 8

PLASTEC  
31442

## NASA Contractor Report 3106

# Analysis of Graphite/Polyimide Rail Shear Specimens Subjected to Mechanical and Thermal Loading

Terry A. Weisshaar and Ramon Garcia  
*Virginia Polytechnic Institute & State University*  
*Blacksburg, Virginia*

Prepared for  
Langley Research Center  
under Grant NGR-47-004-129



National Aeronautics  
and Space Administration

**Scientific and Technical  
Information Office**

1979

Accession For	
NTIS CRA&I	<input checked="checked" type="checkbox"/>
DTIC TAB	<input type="checkbox"/>
Unannounced	<input type="checkbox"/>
Justification _____	
By _____	
Distribution /	
Availability Codes	
Dist	Avail and/or Special
A-1	

## TABLE OF CONTENTS

<u>Section</u>	<u>Page</u>
SUMMARY .....	1
1.0 INTRODUCTION .....	3
2.0 SYMBOLS .....	7
3.0 IDEALIZATION AND ANALYSIS OF RAIL SHEAR TEST SPECIMENS ....	8
3.1 Background - Analysis of Mechanical Loading .....	8
3.2 Background - Analysis of Elevated Temperature Tests .....	12
3.3 Model Idealization and Analysis .....	14
4.0 RESULTS AND DISCUSSION .....	18
4.1 Mechanical Loading .....	18
4.2 Differential Thermal Expansion .....	31
4.2.1 Results for the $[90_{12}]$ Laminate .....	33
4.2.2 Results for the $[0_{12}]$ Laminate .....	38
5.0 CONCLUSIONS .....	47
APPENDIX .....	48
REFERENCES .....	49

## List of Figures

Figure	Title	Page
1	Axially Loaded Rail Shear Test Configuration.....	4
2	Equivalent Loads Acting on the Rails .....	4
3	Finite Element Model of Rail/Specimen Combination.....	15
4	Shear Stress Ratio $\tau/\bar{\tau}$ versus $y/a$ at $x=a/2$ for Four Different Specimens. Aspect Ratio Equals 2.....	19
5	Shear Stress Ratio $\tau/\bar{\tau}$ versus $y/a$ at $x=a/2$ for Three Different Specimens. Aspect Ratio Equals 3.....	21
6	Shear Stress Ratio $\tau/\bar{\tau}$ versus $y/a$ at $x=a/2$ for Three Different Specimens. Aspect Ratio Equals 4.....	22
7	Shear Stress Ratio $\tau/\bar{\tau}$ versus $y/a$ at $x=a/2$ for Three Different Specimens. Aspect Ratio Equals 6.....	24
8	Shear Stress Ratio $\tau/\bar{\tau}$ versus $y/a$ at $x=a/2$ ; $[90_{12}]$ Laminate, Aspect Ratios 6 and 12.....	25
9	Shear Stress Ratio $\tau/\bar{\tau}$ versus $y/a$ at $x=a/2$ ; $[\pm 45_2]_s$ Laminate, Aspect Ratios 6,8,12.....	26
10	Normal Stress Ratio $\sigma_x/\bar{\tau}$ versus $y/a$ at $x/a=0.025$ ; $[90_{12}]$ Laminate, Aspect Ratio Equals 6.....	28
11	Mechanically Loaded Specimen Deformation Pattern; $[90_{12}]$ Laminate; Aspect Ratio Equals 2. Each Grid Section Encloses Four Finite Elements.....	29
12	Mechanically Loaded Specimen Deformation Pattern; $[\pm 45_2]_s$ Laminate; Aspect Ratio Equals 2. Each Grid Section Encloses Four Finite Elements.....	29
13	Mechanically Loaded Specimen Deformation Pattern; $[90_{12}]$ Laminate; Aspect Ratio Equals 4. Each Grid Section Encloses Four Finite Elements.....	30
14	Mechanically Loaded Specimen Deformation Pattern; $[\pm 45_2]_s$ Laminate; Aspect Ratio Equals 4. Each Grid Section Encloses Four Finite Elements.....	30
15	Nondimensional Normal Stresses $\sigma_x/\sigma_T$ and $\sigma_y/\sigma_T$ versus $y/a$ at $x=a/2$ . $[90_{12}]$ Laminate; Specimen Aspect Ratio Equals 2.....	34

<u>Figure</u>	<u>Title</u>	<u>Page</u>
16	Nondimensional Normal Stresses $\sigma_x/\sigma_T$ and $\sigma_y/\sigma_T$ versus $y/a$ at $x=a/2$ . $[90]_2$ Laminate; Specimen Aspect Ratio Equals 4.....	35
17	Nondimensional Normal Stresses $\sigma_x/\sigma_T$ and $\sigma_y/\sigma_T$ versus $y/a$ at $x=a/2$ . $[90]_2$ Laminate; Specimen Aspect Ratio Equals 10.....	36
18	Nondimensional Normal Stress $\sigma_x/\sigma_T$ versus $x/a$ at $y/a=0.025$ . $[90]_2$ Laminate; Specimen Aspect Ratio Equals 10.....	37
19	Nondimensional Normal Stresses $\sigma_x/\sigma_T$ and $\sigma_y/\sigma_T$ versus $x/a$ at $y=b/2$ . $[90]_2$ Laminate, Aspect Ratios 2, 4 and 6.....	39
20	Nondimensional Normal Stresses $\sigma_x/\sigma_T$ and $\sigma_y/\sigma_T$ versus $y/a$ at $x=a/2$ . $[0]_2$ Laminate; Specimen Aspect Ratio Equals 2.....	40
21	Nondimensional Normal Stresses $\sigma_x/\sigma_T$ and $\sigma_y/\sigma_T$ versus $y/a$ at $x=a/2$ . $[0]_2$ Laminate; Specimen Aspect Ratio Equals 4.....	41
22	Nondimensional Stress Distribution $\sigma_y/\sigma_T$ versus $y/a$ at $x=a/2$ . $[0]_2$ Laminate; Specimen Aspect Ratio Equals 10.....	43
23	Nondimensional Normal Stress $\sigma_y/\sigma_T$ versus $x/a$ at $y=b/2$ . $[0]_2$ Laminate, Specimen Aspect Ratios 2, 4, 6, 10.....	44
24	Normal Stress Distribution $\sigma_x/\sigma_T$ versus $x/a$ at $y/a=0.025$ . $[0]_2$ Laminate; Specimen Aspect Ratio Equals 10.....	45

<u>Figure</u>	<u>Title</u>	<u>Page</u>
25	Specimen Deflection Pattern Caused by Heating to Uniform Temperature. $[0_{12}]$ Laminate; Specimen Aspect Ratio Equals 4.....	46
26	Specimen Deflection Pattern Caused by Heating to Uniform Temperature. $[90_{12}]$ Laminate; Specimen Aspect Ratio Equals 4.....	46

## SUMMARY

This report discusses the results of a two-dimensional, linear-elastic, finite element analysis of selected graphite/polyimide rail shear test specimens. The study includes the analysis of mechanical loading and the effect of heating the specimen to a uniform temperature. The presence of specimen free edges and their influence on the accuracy of the rail shear test is discussed. Parameters in this analysis include the length-to-width ratio of the specimen and the ply layup for symmetric, balanced laminates. Results presented include shear and normal stress distributions and the deflection behavior of various specimens caused by the mechanical loading and elevated temperature.

## 1.0 INTRODUCTION

The experimental measurement of the material properties of laminated composite materials is a difficult task. In particular, both the determination of the ultimate strength of a material in shear and the shear modulus pose problems because of the difficulties encountered in attempting to create regions of pure shear within a test specimen. A number of experimental methods exist to determine the shear properties of laminated composites. References 1, 2 and 3 provide discussions and comparisons of the variety of test methods currently in existence.

Perhaps the simplest and least expensive of shear test procedures is the so-called rail shear test. A sketch of a typical two-rail arrangement for this test is shown in figure 1. The test method consists of sandwiching a small, flat, rectangular test specimen between large metallic rails. The attachment of the test specimen to the individual rails is accomplished either by a clamping action provided by bolting the rails to the specimen or by adhesive bonding between the rails and the specimen. The load from the test machine can be introduced into the specimen in one of two ways. One method of load introduction is to apply tensile or compressive loads along the specimen centerline parallel to the rails themselves, as indicated in figure 1. An inplane shear load is transmitted to the test specimen by displacing one rail relative to the other. An alternative method of load application is to apply the loads along a diagonal of the rectangular specimen.

In any test to determine either shear modulus or shear strength of a laminated composite material, a state of uniform shear stress should



① TITANIUM RAIL

② COMPOSITE SPECIMEN

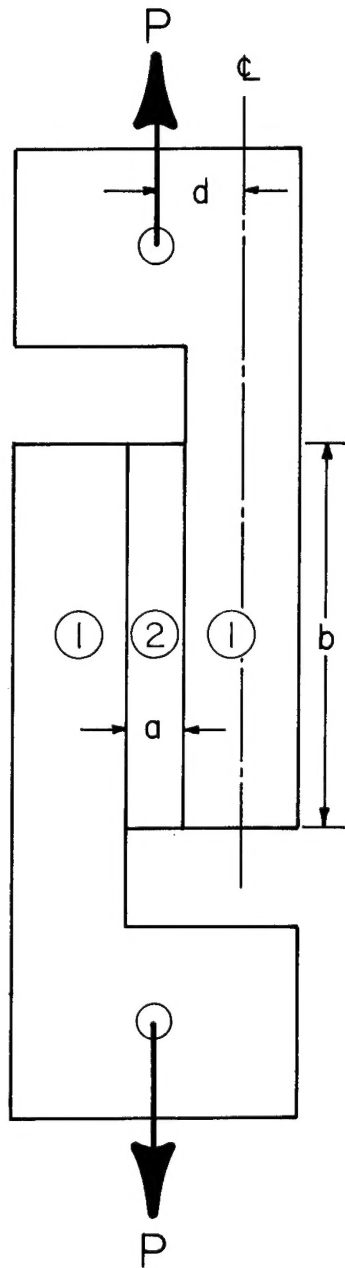


Figure 1 - Axially Loaded Rail Shear Test Configuration

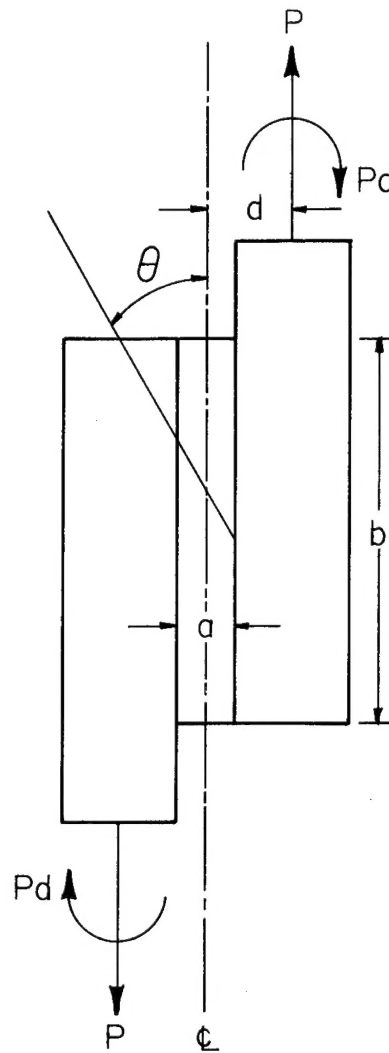


Figure 2 - Equivalent Loads Acting on the Rails

exist within the boundaries of the test specimen. For a flat rectangular specimen, a uniform shear state can be imposed only by loading all four boundaries; such simultaneous loading of the specimen boundaries is not present in the standard rail shear test. A result of the rail shear type of loading is that two parallel edges of the specimen are loaded while the remaining two parallel edges remain stress free. It has been shown (ref. 4) that the presence of these free edges gives rise to edge zones in which the inplane shear stress varies greatly. Accompanying these shear stress variations are normal stresses that ensure stress equilibrium. The fact that normal stresses are developed within the specimen by the loading shown in figure 1 has given rise to criticism of the use of the rail shear test to determine laminate properties (ref. 5). These normal stresses may cause undesirable occurrences such as debonding of the specimen/rail interface or failure of the specimen near its corners due to mechanisms other than shear initiated failure. In addition, the presence of a nonuniform shear stress distribution within the specimen may lead to considerable error in the determination of the shear modulus.

Previous studies, such as those by Whitney, Stansbarger and Howell (ref. 5) and Whitney (refs. 6,7), have shown that the nonuniformity of the stresses in the edge zone, and thus the deviation from a state of pure shear within the specimen, is governed by such factors as the specimen length-to-width ratio (also referred to as the aspect ratio,  $b/a$  in figure 2) and the laminate layup.

An additional problem appears when testing specimens at elevated

temperatures. Because the rails and the composite specimen are made of dissimilar materials, thermally induced stresses are caused by differential thermal expansion. This problem is discussed by Bergner, Davis and Herakovich (ref. 3). Results of a finite element analysis of a large length-to-width ratio specimen are presented in this latter report; these results show that elevated temperatures may produce additional large normal stresses near the test specimen corners. The analytical results presented in reference 3 are limited in scope since the effect of specimen aspect ratio on test validity is not considered.

In an effort to obtain more comprehensive knowledge and understanding of the stress fields that arise in a rail shear test with loading of the type illustrated in figure 1, both at room temperature and at elevated temperature, a series of analytical studies using finite element models was performed. The analyses and results presented in this report are those that consider a two-dimensional, balanced, symmetrical-ply, rail shear test specimen with flexible rails. Classical linear-elastic, laminated plate theory is used for the finite element model. Specimen aspect ratios of between 2 and 12 are considered. Results presented include shear and normal stress distribution information at various positions on the rail shear specimen, both for mechanical and thermal loading. For the mechanical loading case, the laminates considered are  $[0]_2$ ,  $[90]_2$ ,  $[90/\pm 45/0]_s$  and  $[\pm 45]_2$  layups, while the thermal load cases include only the  $[0]_2$  and  $[90]_2$  laminates. From these results, conclusions are drawn about the acceptability of the rail shear test as an experimental tool for shear testing of composites.

## 2.0 SYMBOLS

Definitions of the major symbols used in this report are given in this section. Symbols not having general use are defined as they are introduced. The units used for physical quantities are given in the International System of Units (SI), except where noted.

$a, b$	Specimen width and length respectively (figure 2).
$E_0$	Modulus of elasticity in the laminate $0^\circ$ direction.
$P$	Test machine load applied to rail (figure 1).
$t$	Test specimen thickness.
$\Delta T$	Change in temperature.
$\alpha_r$	Coefficient of thermal expansion of the rail.
$\alpha_s$	Coefficient of thermal expansion of the specimen in the $0^\circ$ direction.
$\Delta\alpha$	$\alpha_r - \alpha_s$ , Eqn. 2.
$\tau$	Shear stress in the x-y coordinate system.
$\bar{\tau}$	Average shear stress, $\bar{\tau} = P/bt$ .
$\sigma_T$	Reference stress for thermal stress results, Eqn. 1.

### 3.0 IDEALIZATION AND ANALYSIS OF RAIL SHEAR TEST SPECIMENS

#### 3.1 Background - Analysis of Mechanical Loading

The interest in this report is focused upon the two-dimensional stress distributions in flat rectangular specimens that have balanced, symmetrical-ply, laminated composite material and are subjected to in-plane shear loading. Furthermore, the mechanical loading may occur both at room temperature and at elevated temperature. Because the analytical model to be discussed is linear elastic, superposition principles apply. Thus the overall problem may be subdivided into two parts: (1) mechanical loading with no temperature effects included; and (2) the introduction of temperature effects with no external load.

The interest in the mechanical loading of flat rectangular plates by inplane shear loads of the type found in rail shear testing extends back to the early part of this century. In 1912, Coker (ref. 4) conducted photoelastic experiments to determine the effect of specimen aspect ratio (length-to-width ratio) on the shear stress distribution in isotropic flat plates with parallel edges subjected to edge shear, a loading that is nearly identical to that imposed during the rail shear test. For small aspect ratio specimens, Coker determined a shear stress distribution, along the specimen centerline parallel to the applied shear load, much like the parabolic distribution that is predicted from elementary, strength of material, beam theory. This parabolic distribution of shear stress was found to change as the specimen aspect ratio increased. Instead of a single maximum stress, as occurs for a parabolic shear stress

distribution, plates with larger aspect ratios (of the order of 4) exhibit two shear stress maxima, symmetrically located about the plate center. These maxima are located at a distance of about  $3/4$  of an edge width from the free edges of the plate specimen. Coker further showed, by photoelastic experiment, that the shear stress remains at a reasonably constant value in the interior of the plate. This latter result of Coker's work is frequently cited as justification for the use of large aspect ratio, rail shear specimens for testing of isotropic materials.

In 1923, Inglis (ref. 8) published an analytical study of Coker's experimental work. In this study, Inglis used a classical stress function approach to formulate and to solve, approximately, the theory of elasticity problem for a linear elastic, isotropic material with two parallel edges loaded in shear and the other two edges free. The loaded boundaries are assumed to be rigid. A series solution was obtained that is quite accurate in regions away from the plate corners. Inglis found that a large stress, normal to the boundary loaded in shear, appears near the corners of the plate. This normal stress has a magnitude four times that of the average inplane shear stress,  $\bar{\tau}$ , applied to the plate boundaries. It was noted that this stress concentration factor of four is somewhat inaccurate because of the truncation of the assumed series solution.

The analysis of two other problems related to the rail shear test received considerable attention in the late 1930's and during the 1940's. The first problem, that of shear lag in reinforced sheet-stringer

construction, was the subject of a number of papers and reports (see Kuhn, ref. 9). The shear lag problem approximates the theory of elasticity problem in which axial loads are transferred from flexible longitudinal stiffeners to thin sheets of shear web material attached to the stiffeners. The key assumption of shear lag analysis is that the transverse stiffness of the specimen is infinite. The important finding of these shear lag analyses for isotropic materials is that the load transfer, or load diffusion, from flexible stiffeners to the shear web material produces regions of non-uniform stress at the panel ends where the axial load is introduced. This non-uniform stress distribution decays exponentially with distance if the panel is long enough; the argument of the exponential decay function is related to stiffener and sheet material properties and sheet geometry. In particular, for isotropic materials the factor  $(G/E)^{1/2}$  is found to be a parameter in this exponential argument. The parameter  $G$  is the shear modulus of the material while  $E$  represents the modulus of elasticity in the direction of the applied axial load.

Hildebrand (ref. 10) presents several exact solutions to the differential equations that govern shear-lag in orthotropic panels that are assumed to be rigid in the transverse direction (perpendicular to the applied axial load direction). While this latter assumption precludes the use of these results for the rail shear problem, Hildebrand's results show the exponential decay character of the stresses caused by this type of loading.

A field of study with characteristics related to the rail shear test is found in the area of bonded joints. In particular, the work of Goland and Reissner (ref. 11) predicts normal stresses at corners of

bonded lap joints. These "tearing" stresses are set up in the adhesive as a result of the eccentricity of the loading on the lap joint. Goland and Reissner make certain simplifying assumptions which cause their results to be not strictly applicable for analysis of the rail shear test. For instance, the adherends are assumed to be relatively flexible and adhesive flexibility is ignored in a direction transverse to the load direction. Their studies do, however, reveal that large tearing stresses normal to the applied load direction may be expected in the vicinity of the joint edges. In a rail shear test, these joint edges correspond to the rail shear specimen corners.

More recently, the application of the rail-shear test to advanced composite materials has received considerable attention. Whitney, Stansbarger and Howell (ref. 5) and Whitney (references 6, 7) have studied the rail shear test in some detail. Reference 6 presents a detailed analysis of the stresses in a symmetrical, balanced-ply, laminated plate loaded by inplane shear along two parallel edges that are rigid but displace relative to each other to cause shear in the specimen. One potential difficulty with the analysis presented is that a Fourier series solution for the displacement field was used to solve the problem. The series solution used is discontinuous at the free edges; thus, the solution discontinuity at the edge may be masking the free edge effects. In reference 7, test results are presented for a rectangular orthotropic rail shear specimen clamped to metallic rails, while reference 5 summarizes much of the work presented in references 6 and 7.

Bergner, Davis and Herakovich (ref. 3) present a limited analytical study of the rail shear test with composite materials. Reference 3 is



significant because, unlike the differential equation approach used in previous studies, the authors use a finite element analysis for the study of rail shear testing both at room temperature and also with temperature effects. Their results show the superiority of the finite element approach over the Fourier series solution.

### 3.2 Background - Analysis of Elevated Temperature Tests

The elevated temperature rail shear test has not been examined in great detail. Reference 3 presents an analysis of the stresses occurring in a rail shear test specimen with flexible rails when the temperature is lowered  $316^{\circ}\text{C}$  ( $600^{\circ}\text{F}$ ). The results of that study show that regions of large normal stress occur in the specimen corners as the temperature is changed; this thermal stress is found to be significant.

Two previous studies consider a problem that is similar to that encountered in elevated temperature rail shear testing. Aleck (ref. 12) has analyzed the thermal stresses in a rectangular plate of isotropic material in which one edge is cemented to a perfectly rigid plane while the other three edges are allowed to be free. The solution of this problem with energy methods yielded a solution that is suspect, in that the stress functions used to approximate the solution are somewhat simplified and thus inadequate to represent the solution.

A thermal stress study by Kobatake and Inoue (ref. 13) concerns a linear elastic, isotropic rectangular plate, two of whose parallel edges have been fixed to rigid planes before heating is introduced. The study presented in reference 13 indicates that, due to the restrained thermal expansion, large normal stresses and shear stresses appear near

the plate corners. However, the magnitude of these stresses tends to decrease rapidly with distance away from the free edges (distances that are slightly greater than an edge width of the plate). Unfortunately, boundary conditions are applied to the plate that lead to edges free of stress normal to the interface. As a result of this, the stress distributions near the interface, presented in reference 13, are not correct for the present problem. Nevertheless, reference 13 indicates that sizable shear and normal stresses near the specimen corners may be caused by constrained expansion of the rails and the specimen during an elevated temperature rail shear test. For instance, the maximum value of shear stress computed near the specimen corners is, for their isotropic material,  $\tau = 0.645 E(\Delta\alpha) (\Delta T)$ , where  $E$ ,  $\Delta\alpha$  and  $\Delta T$  represent the modulus of elasticity, the difference between the values of the coefficients of thermal expansion of the rails and specimen, and the change in temperature, respectively. Of further significance, is that the shear stress caused by thermal expansion is minimal at a distance of two plate edge widths into the plate from the free edges and, at one width, has a value of only about 25% of the maximum value given above. Symmetry considerations indicate that the shear stress  $\tau$  is zero along both specimen axes of symmetry.

A conclusion to be drawn from reference 13 is that, during a rail shear test at elevated temperature, stresses caused by thermal expansion probably will not affect significantly the determination of the shear modulus. However, the shear and normal stresses generated near the corners of the specimen at the specimen/rail interface may

lead to premature failure of the specimen at or near this interface. For adhesively bonded, rail/shear specimens, these stresses may cause the bond itself to fail due to insufficient strength.

The studies previously cited provide guidance for the idealization and stress analysis of the rail shear test specimen. These studies show that a finite element model provides a simpler and more accurate analytical tool for the study. In addition, the flexibility of the rails should be considered. Finally, careful attention must be given to the model idealization in the vicinity of the specimen corners where large stress gradients will occur. The next section describes the finite element model used for this study.

### 3.3 Model Idealization and Analysis

The formulation of an accurate but economical (in terms of computer time) finite element model of a rail/specimen combination, such as shown in figure 1, requires that some assumptions be made about the expected physical behavior of the test specimen and its rails under the applied load. The idealized model chosen to approximate this behavior focuses attention on the two-dimensional displacement and stress behavior of the composite test specimen, while retaining the important influence of the axial flexibility and bending flexibility of the two titanium rails.

Consider figure 3, in which is shown a typical finite element idealization of the rail shear test configuration used in this analysis. The flat rectangular specimen itself is modelled as an assemblage of planar, rectangular finite elements whose material behavior is linear elastic, but anisotropic. The rails are titanium, chosen because of

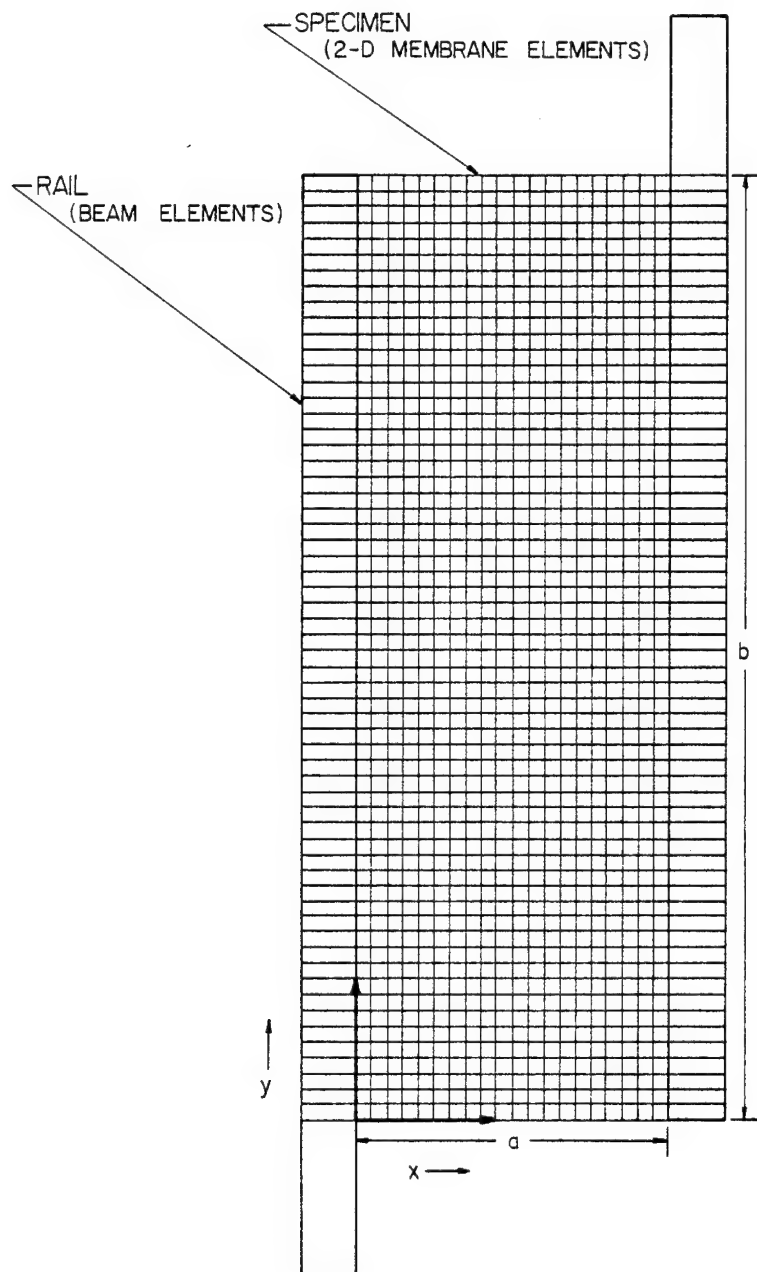


Figure 3 - Finite Element Model of Rail/Specimen Combination.  
 (Note that x-y coordinate origin is in the lower left corner of the specimen.)

their characteristic small coefficient of thermal expansion. These rails are represented by beam elements with a straight elastic axis in the plane of the specimen and parallel to the y-axis of the specimen in figure 3.

Although the load from the test machine is applied along the specimen centerline parallel to the y-axis in figure 3, the mathematical idealization employs a statically equivalent load combination consisting of a concentrated force and moment applied to the end of a straight beam that simulates the rail. This load set is illustrated in figure 2.

Since the finite element analysis involves a numerical representation of the structure, while the interpretation of the analysis results is best accomplished in nondimensional parameter form, consistent parameters are assigned to the models so that some parameters are fixed while others are varied. From the literature previously cited, it is expected that two effects will affect the diffusion of the axial loads from the rails into the test specimen. These effects are the presence of the specimen free edges and the elastic interaction between the rails and the specimen. For these reasons, the cross-sectional area and shape of the rails was held fixed, as was the specimen width, the dimension "a" in figure 2. For aspect ratio studies, the dimension b was varied to achieve the proper b/a ratio.

Idealized structural models with geometries of the type shown in figure 3 were developed and analyzed using the SPAR computer program (ref. 14) at the NASA/Langley Research Center. The results of these analyses are described in Section 4.0. The geometrical parameters and

material properties of the rails and the graphite/polyimide material are given in the Appendix.

## 4.0 RESULTS AND DISCUSSION

The importance of the rail shear test specimen aspect ratio and the effect of the laminate layup on the stress field present during testing have been noted in the previous discussion. To study the effects of aspect ratio and laminate layup, several different aspect ratios were considered for four types of laminates. The laminates are composed of multiple layers of graphite/polyimide material. The laminates considered are:

- (1) a  $[0_2]$  laminate,
- (2) a  $[90_2]$  laminate,
- (3) an 8-layer  $[\pm 45_2]_s$  laminate,
- (4) an 8-layer  $[90/\pm 45/0]_s$  laminate.

The reference position for the measurement of the fiber angle  $\theta$  is illustrated in figure 2.

### 4.1 Mechanical Loading

Considering first a specimen with an aspect ratio of 2, it is seen in figure 4 that laminate construction greatly affects the shear stress distribution along the centerline parallel to the y-axis. Figure 4 displays the laminate shear stress versus distance from the free edge; this latter distance is nondimensionalized with respect to the specimen width. The shear stress in the laminate is nondimensionalized with respect to the average value of the shear stress, computed as  $\bar{\tau} = P/bt$ . Since these distributions of shear stress are symmetrical about  $y = b/2$ , only the distributions present in half the specimen are shown. It must be noted here that the stresses shown throughout this report are the result of taking the resultant inplane forces per

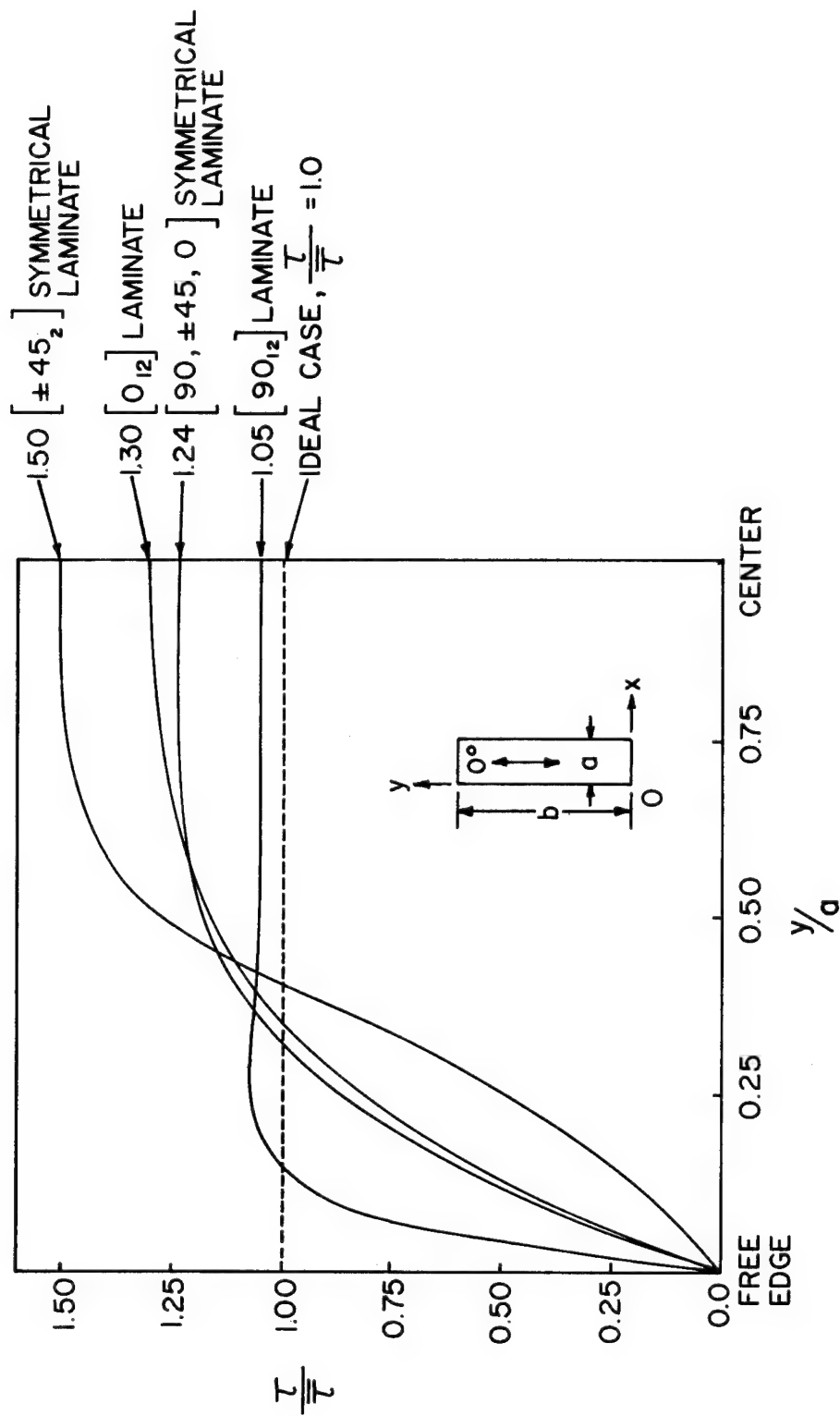


Figure 4 - Shear Stress Ratio  $\tau/\bar{\tau}$  versus  $y/a$  at  $x=a/2$  for Four Different Specimens. Aspect Ratio Equals 2.



unit length,  $N_x$ ,  $N_y$  and  $N_{xy}$  present in the laminate and dividing by the laminate thickness  $t$ . Thus, depending upon the laminate layup, the stresses in the individual lamina may be different than those values given in the ensuing discussion.

For the  $[90]_2$  laminate, the discrepancy between the actual value of shear stress  $\tau$  and the average value of shear stress,  $\bar{\tau}$ , is seen to be 5% at the specimen center. The discrepancy is 50% for the  $[\pm 45]_2$  laminate. In addition, the shapes of the nondimensional shear stress distributions are different. The shape of the  $\tau/\bar{\tau}$  distribution for the  $[0]_2$  laminate and that for the  $[90/\pm 45/0]_s$  laminate more nearly resemble the parabolic distributions observed by Coker for isotropic specimens with the same aspect ratio.

When the aspect ratio of the specimen is increased to 3, the disparity between the true shear stress and the average shear stress at the specimen center is less than that previously seen, as is shown in figure 5. The discrepancy at the specimen center between the average shear stress and the true shear stress is as little as 3% for the  $[90]_2$  laminate. The  $[\pm 45]_2$  laminate still shows a 27% difference at the center. The data for the  $[90/\pm 45/0]_s$  laminate is not shown because its behavior so closely approximates that of the  $[0]_2$  laminate.

Figure 6 illustrates the effect on the shear stress distribution of increasing still further the specimen aspect ratio to 4. Differences between the average shear stress  $\bar{\tau}$  and the true shear stress  $\tau$  at the specimen center decrease from those shown in figure 5 and are between 2% and 17%. In addition, this figure clearly shows the presence of a

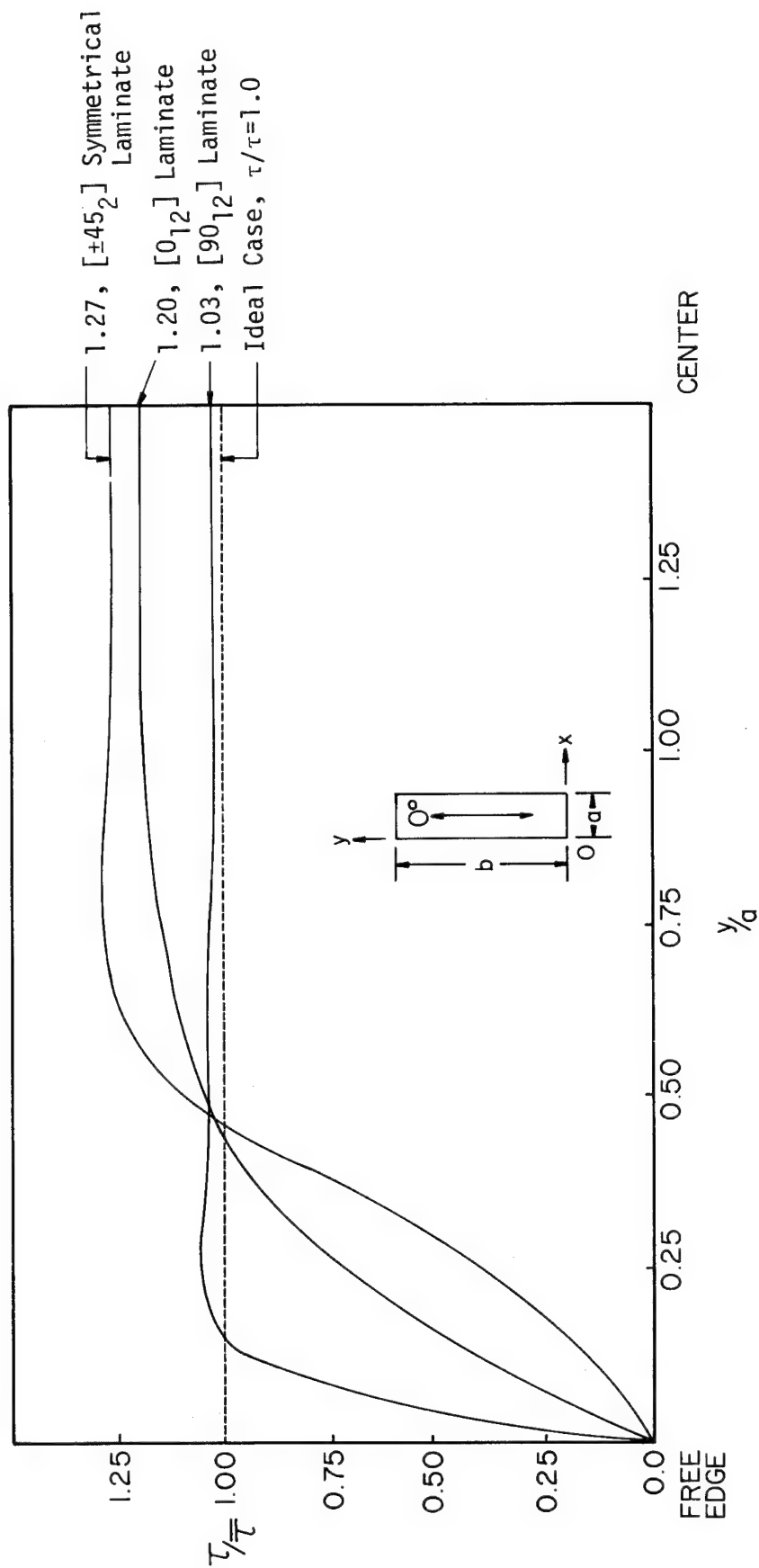


Figure 5 - Shear Stress Ratio  $\tau/\bar{\tau}$  versus  $y/a$  at  $x=a/2$  for Three Different Specimens. Aspect Ratio Equals 3.

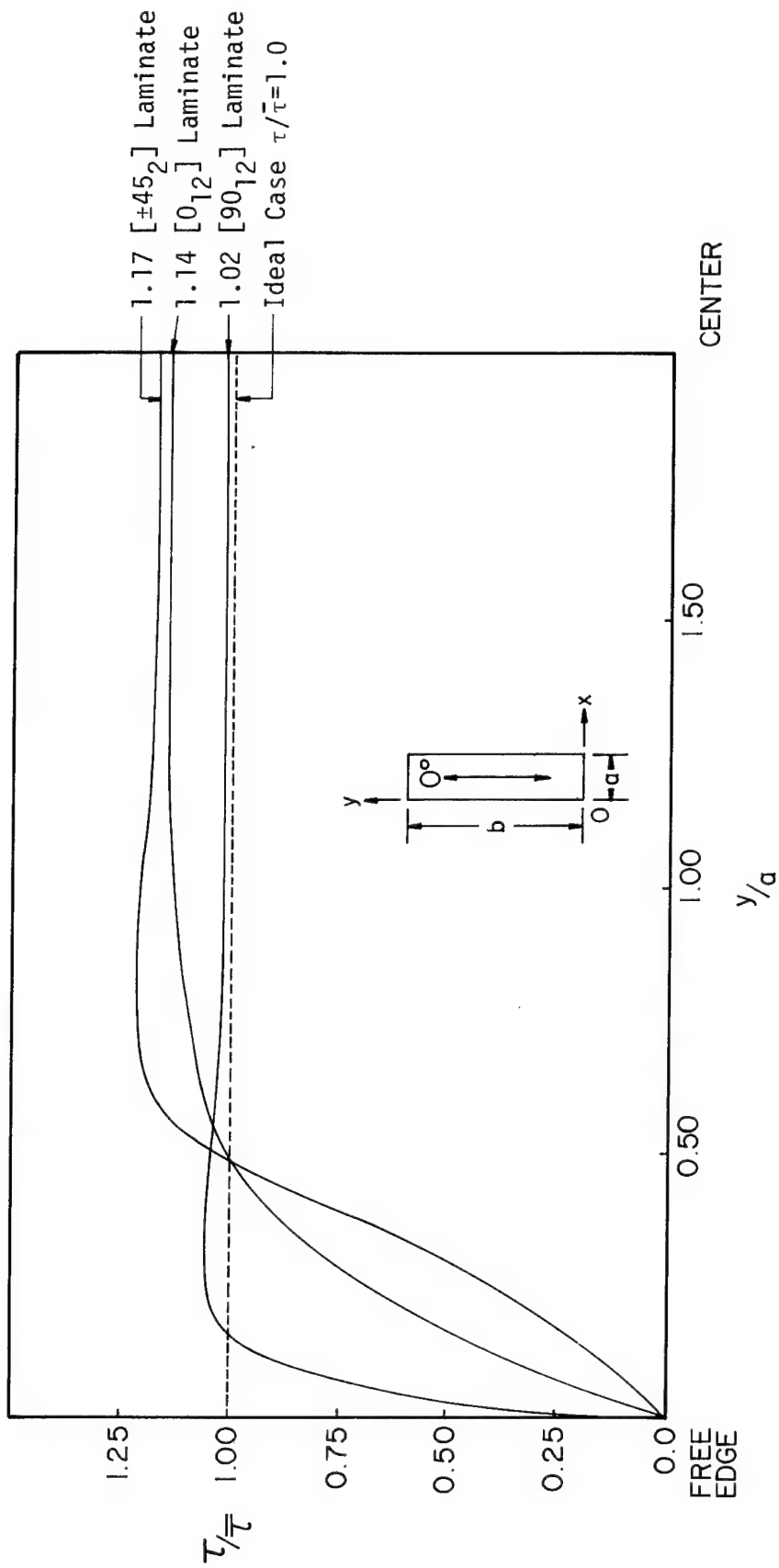


Figure 6. - Shear Stress Ratio  $\tau/\bar{\tau}$  versus  $y/a$  at  $x=a/2$  for Three Different Specimens. Aspect Ratio Equals 4.

local maximum shear stress, a type of shear stress distribution similar to that noted by Coker in his results for specimens with a similar aspect ratio.

By further increasing the aspect ratio from 4 to a value of 6, the difference between the average shear stress and the true shear stress narrows even more. Figure 7 shows these differences at the specimen center to be from between 1% and 8%, depending upon the type of laminate.

To illustrate further the effect of changing specimen aspect ratio upon the shear stress distribution within the specimen, let us focus attention upon two laminates, the  $[90_{12}]$  laminate and the  $[\pm 45_2]_S$  laminate. These laminates are chosen because of the contrasting behavior of their shear stress distributions.

Figures 8 and 9 illustrate the behavior of the shear stress distribution for these two laminates as specimen aspect ratio is increased from 6 to 12. In figure 8, it is seen that doubling the aspect ratio of the  $[90_{12}]$  specimen from 6 to 12 changes very little the shear stress distribution along the specimen centerline. The shear stress ratio  $\tau/\bar{\tau}$  at the specimen center is less than unity for an aspect ratio of 12. As a consequence, the maximum value of the shear stress, found near the free edge, increases as the aspect ratio increases. However, the change in these maximum values is slight.

Figure 9 shows shear stress distributions for the  $[\pm 45_2]_S$  laminate that are in marked contrast to those seen in figure 8. As specimen aspect ratio increases, a very pronounced increase in the maximum shear stress, occurring near the free edge, is seen. Even so, the shear stress ratio  $\tau/\bar{\tau}$ , present at the specimen center, is very nearly unity.

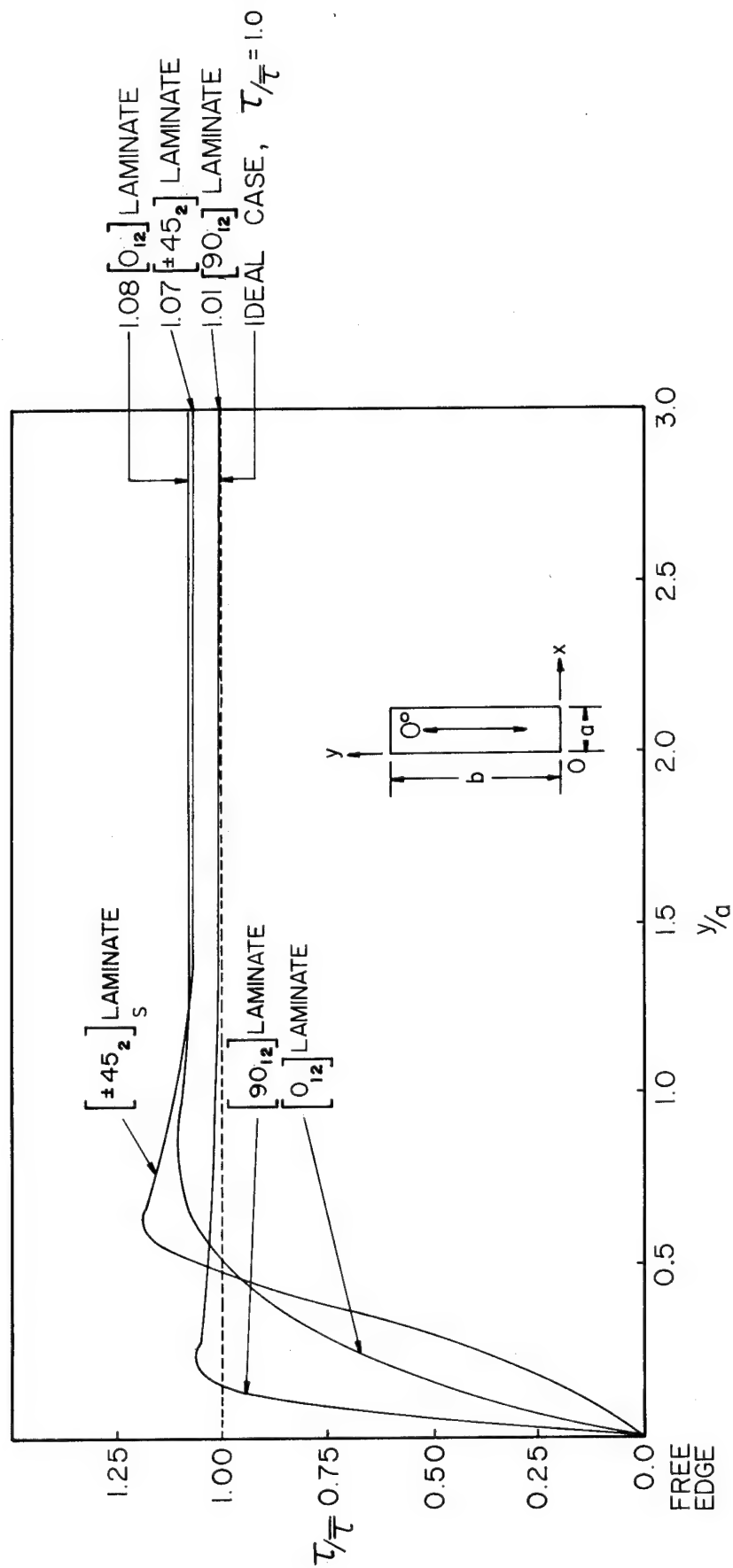


Figure 7 - Shear Stress Ratio  $\tau/\bar{\tau}$  versus  $y/a$  at  $x=a/2$  for Three Different Specimens. Aspect Ratio Equals 6.

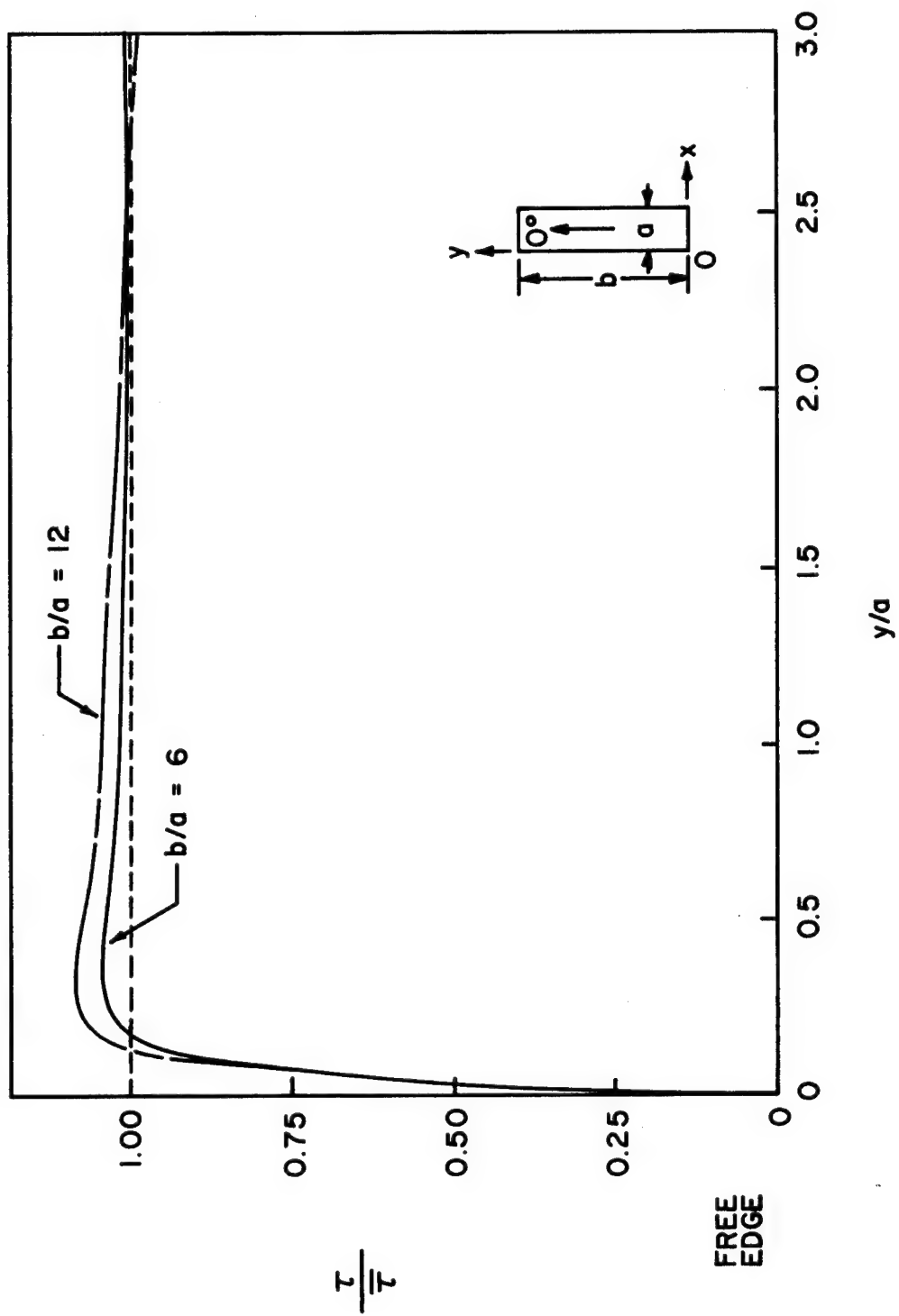


Figure 8 - Shear Stress Ratio  $\tau/\bar{\tau}$  versus  $y/a$  at  $x=a/2$ ;  $[90_{12}]$  Laminate, Aspect Ratios 6 and 12.

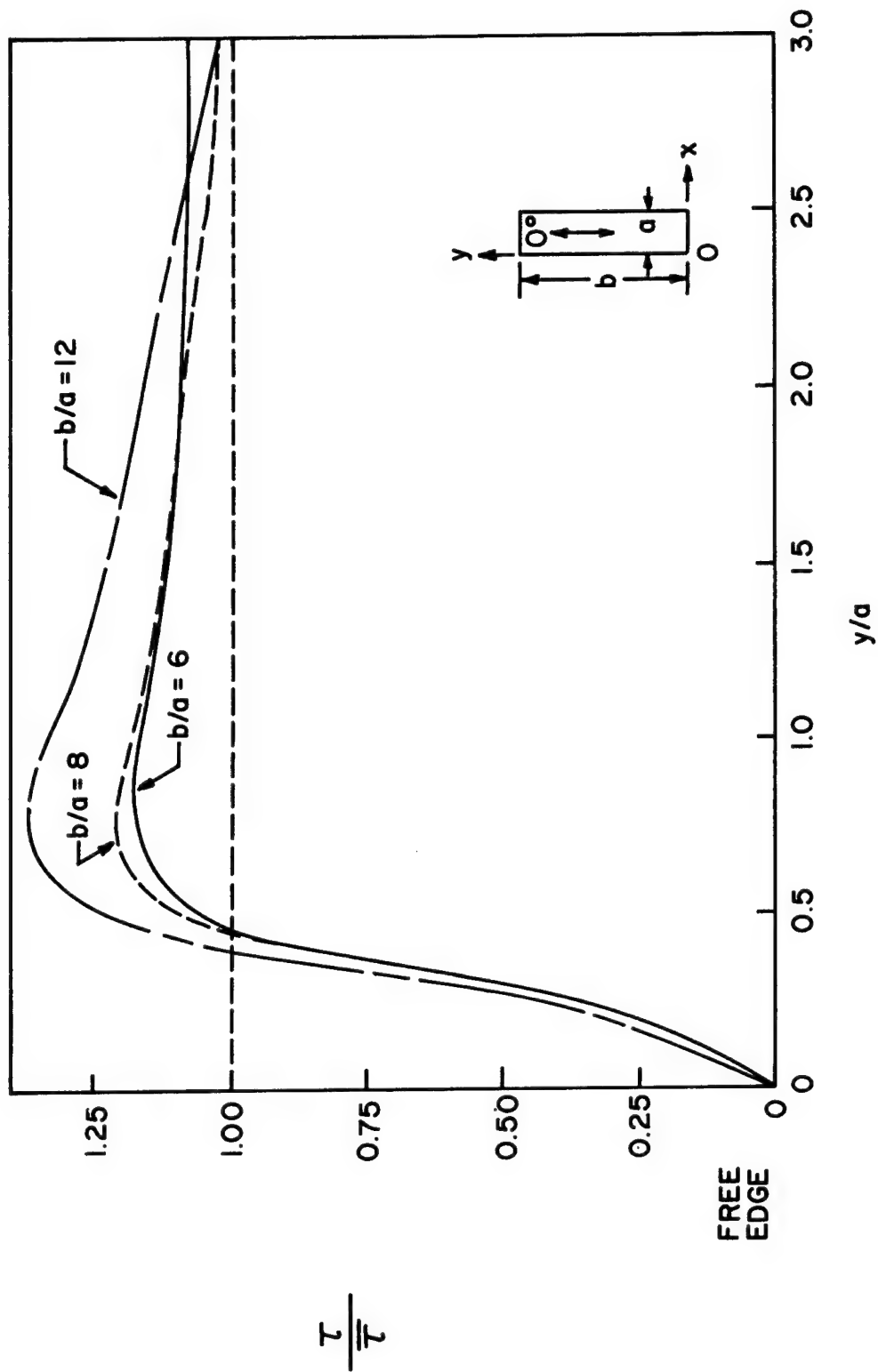


Figure 9 - Shear Stress Ratio  $\tau/\bar{\tau}$  versus  $y/a$  at  $x=a/2$ ;  $[\pm 45_2]_s$  Laminate, Aspect Ratios 6, 8, 12.

The appearance of a nonuniform shear stress field within the specimen gives rise to normal stress fields. An example of the  $\sigma_x$  stress distribution that occurs is shown in figure 10. In figure 10, data taken from the finite element analysis of a  $[90_{12}]$  laminate with aspect ratio 6 is displayed. This curve represents the normal stress  $\sigma_x$  (normalized with respect to the average shear stress  $\bar{\tau}$ ), occurring at the centers of finite elements used in the specimen model, adjacent to the rail/specimen interface. For this model, the locus of these points is a line at a distance  $0.025a$  from this interface. The stress distribution shown in figure 10 illustrates the large stress concentrations present at the specimen corners. The normal stress is seen to decrease rapidly with distance from the free edge.

The ratio  $\sigma_x/\bar{\tau}$  calculated near the corners of specimens is shown in the table below for several aspect ratios.

Aspect Ratio	Location of Data (x,y)	$[90_{12}]$	$[\pm 45_2]_s$	$[0_{12}]$	$[90/\pm 45/0]_s$
2	(0.025a,0.025a)	6.97	2.31	3.05	3.35
3	(0.025a,0.025a)	6.95	2.03	2.88	3.21
4	(0.025a,0.067a)	6.14	1.84	2.63	2.97
6	(0.025a,0.025a)	7.51	2.07	2.83	3.40
10	(0.05a,0.025a)	8.46	2.44	2.73	3.97

STRESS CONCENTRATION FACTORS  $\sigma_x/\bar{\tau}$  NEAR SPECIMEN CORNERS



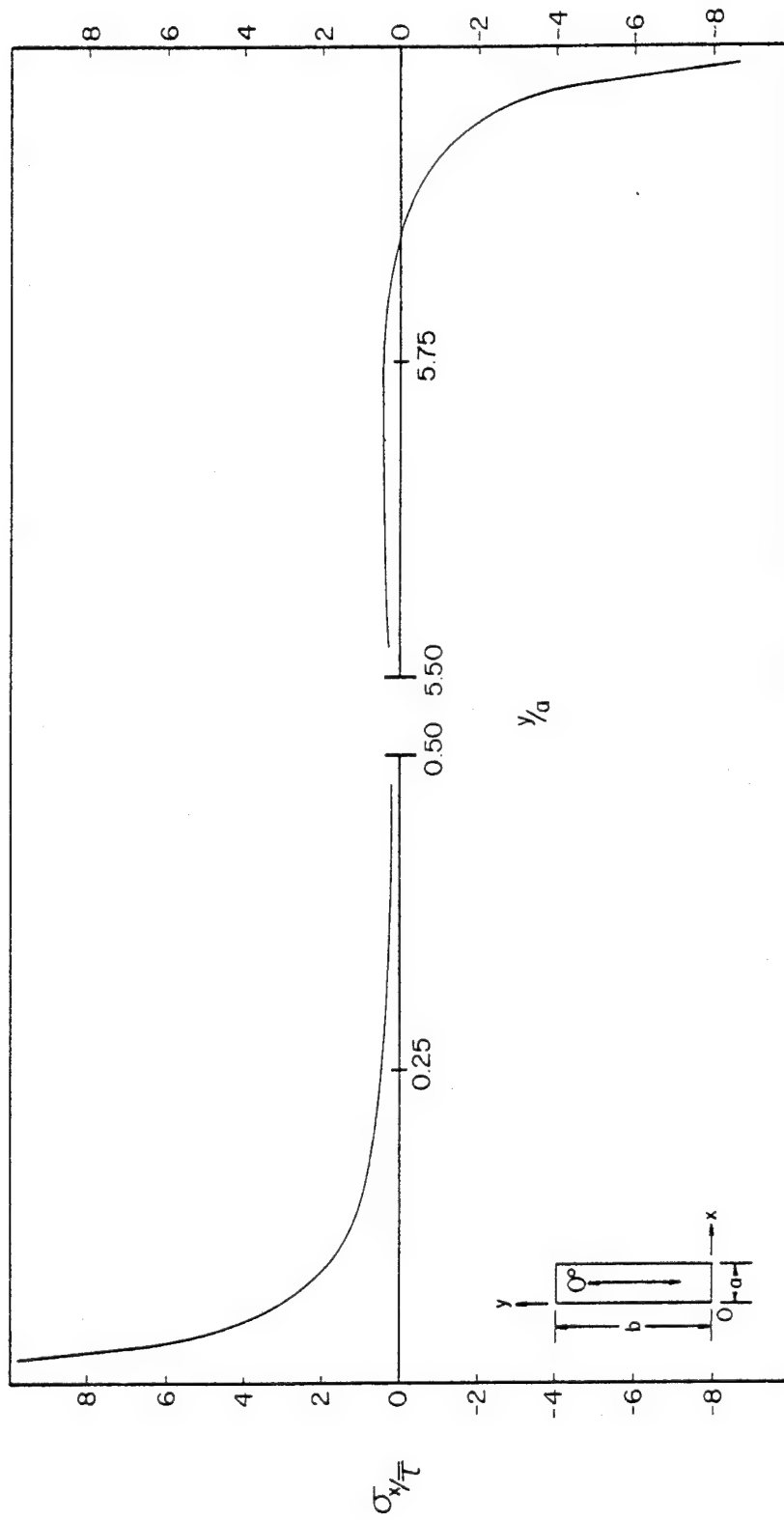


Figure 10 - Normal Stress Ratio  $\sigma_x/\tau$  versus  $y/a$  at  $x/a=0.025$ ;  $[90_{12}]$  Laminate, Aspect Ratio Equals 6.

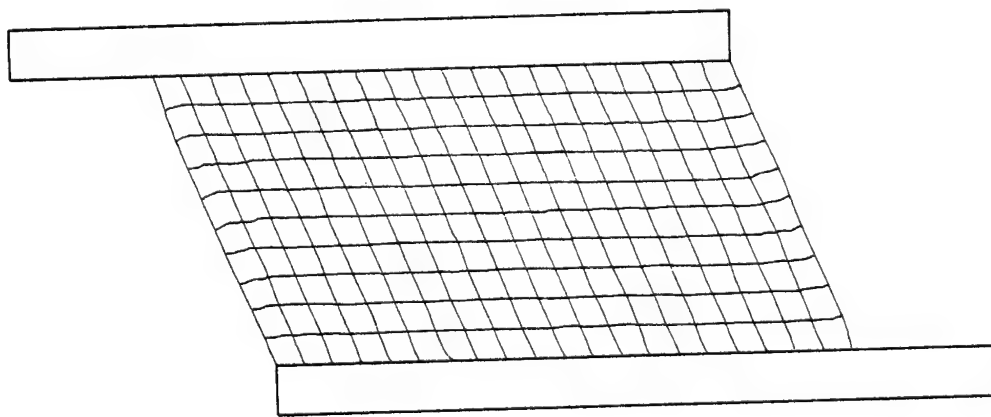


Figure 11 - Mechanically Loaded Specimen Deformation Pattern;  $[90_{12}]$  Laminate; Aspect Ratio Equals 2. Each Grid Section Encloses Four Finite Elements.

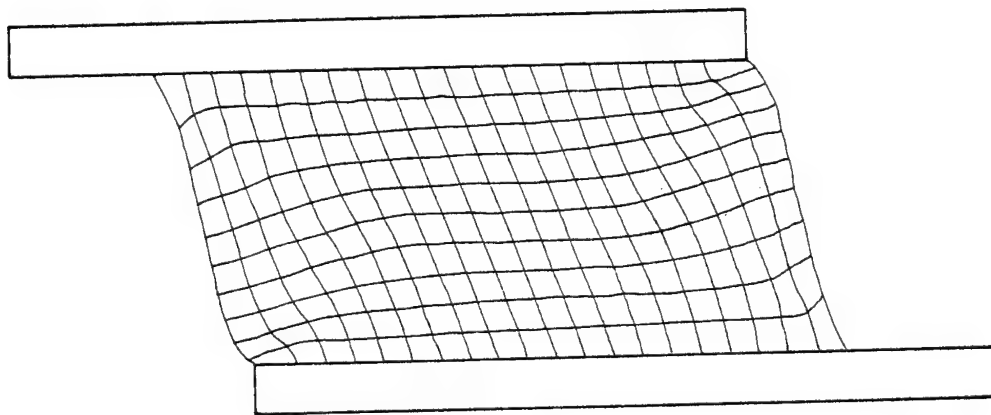


Figure 12 - Mechanically Loaded Specimen Deformation Pattern;  $[\pm 45_2]_s$  Laminate; Aspect Ratio Equals 2. Each Grid Section Encloses Four Finite Elements.

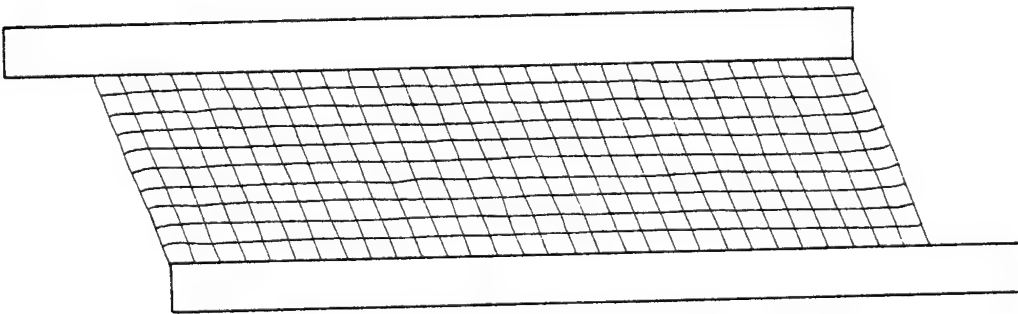


Figure 13 - Mechanically Loaded Specimen  
Deformation Pattern;  $[90_{12}]$   
Laminate; Aspect Ratio Equals  
4. Each Grid Section Encloses  
Four Finite Elements.

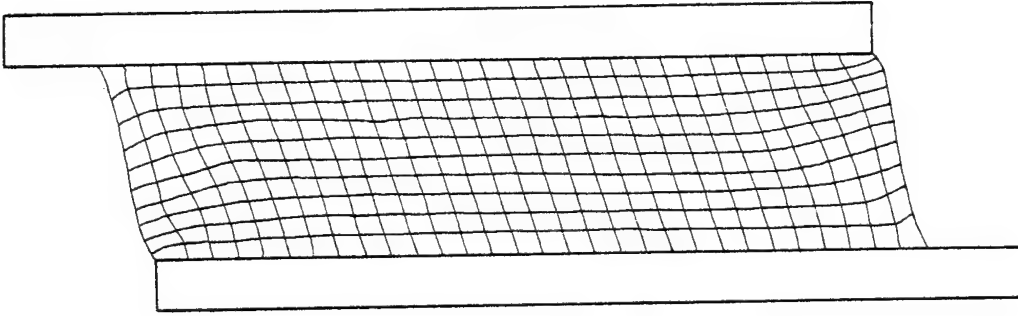


Figure 14 - Mechanically Loaded Specimen  
Deformation Pattern;  $[\pm 45_2]_S$   
Laminate; Aspect Ratio Equals  
4. Each Grid Section Encloses  
Four Finite Elements.

From this table of values it is seen that the ratio  $\sigma_x/\bar{\tau}$  near a specimen corner can be quite large, particularly in the case of the  $[90_2]_s$  specimen. Note that the data displayed in the table are not given at exactly the same x,y positions due to differences in finite element mesh sizes for the various aspect ratios.

To complete the presentation of the effects of mechanical loading upon the rail shear specimen, figures 11 through 14 are presented; these figures contrast the displacement behavior of the  $[90_2]_s$  laminate with the  $[\pm 45_2]_s$  laminate for aspect ratios of 2 and 4.

#### 4.2 Differential Thermal Expansion

Because of the mismatch between coefficients of thermal expansion, the heating or cooling of a rail shear specimen will cause stresses to develop in the rails and the test specimen. Fortunately, the geometrical symmetry of the specimen and the rails and the nature of the thermal loading preclude the development of a shear stress  $\tau$  along either of the centerlines of the specimen. For this reason, the experimental determination of the shear modulus is unlikely to be affected by temperature if the shear strain is measured at the specimen center. However, near the corners of the specimen, sizable thermal stresses may develop, stresses that may cause experimental error when testing for the ultimate strength of the laminate in shear.

The finite element models used in this portion of the study assume the rail and specimen to be heated to a uniform temperature. In addition, the specimen and the attached rails are free to expand laterally. The finite element idealizations used for the thermal

expansion study are identical to those described in the previous study of mechanical loading.

To illustrate the response of an orthotropic test specimen to a uniform temperature increase, results are presented for two test specimens, the  $[0_{12}]$  and  $[90_{12}]$  laminates; four aspect ratios are analyzed. Nondimensionalization of the results is accomplished by dividing the thermally induced stress at any point on the laminate by a reference stress  $\sigma_T$ , given by the expression

$$\sigma_T = E_0 (\Delta\alpha) (\Delta T) \quad (1)$$

In Eqn. 1,  $E_0$  is the modulus of elasticity of the specimen in the  $0^\circ$  direction of the laminate, while  $\Delta\alpha$  is given by the relationship

$$\Delta\alpha = \alpha_r - \alpha_s \quad (2)$$

In Eqn. 2,  $\alpha_r$  is the coefficient of thermal expansion of the rails, while  $\alpha_s$  is the coefficient of thermal expansion of the specimen in the  $0^\circ$  direction.  $\Delta T$  is defined as the temperature change from the zero strain condition. Note that the value of  $\sigma_T$  depends upon the specimen being studied.

A physical interpretation of  $\sigma_T$  is that it is the value of the compressive stress necessary to keep the extensional strain in the  $0^\circ$  direction of the specimen equal to zero for a material with a coefficient of thermal expansion of  $\Delta\alpha$  and a temperature change  $\Delta T$ . Since no such stress can be applied to the specimen, because of the two stress free edges, the specimen normal stresses near these edges

in the  $y$  direction will differ from this value, but it will be shown that the  $\sigma_y$  stresses will approach this  $\sigma_T$  value over the central region of the specimen if the aspect ratio is large enough.

#### 4.2.1 Results for the $[90_{12}]$ Laminate

Shown in figure 15 are the normalized distributions of stress  $\sigma_x/\sigma_T$  and  $\sigma_y/\sigma_T$  that occur along the line  $x=a/2$  for a  $[90_{12}]$  laminate with an aspect ratio of 2. If the specimen is heated, the stress  $\sigma_y$  will attain a maximum compressive value near the center of the specimen. At the center of the free edge of the specimen, the normal stress  $\sigma_x$  will have a large tensile value, a value that declines rapidly with distance away from the free edge. It should be noted that the reference stress  $\sigma_T$  for this laminate will be negative for an increase in temperature, due to the fact that  $\alpha_s$  exceeds  $\alpha_r$ .

Figures 16 and 17 show the behavior of the normal stresses  $\sigma_x$  and  $\sigma_y$ , at  $x=a/2$ , for the  $[90_{12}]$  laminate with specimen aspect ratios of 4 and 10, respectively. These stresses, nondimensionalized with respect to  $\sigma_T$  for this laminate and plotted against  $y/a$ , behave in a manner similar to those plotted in figure 15.

The behavior of the normal stress  $\sigma_x$  near the free edge of a  $[90_{12}]$  specimen with an aspect ratio of 10 is illustrated in figure 18. In this figure, the quantity  $\sigma_x/\sigma_T$  at the position  $y/a=0.025$  is graphed versus  $x/a$ . This figure shows that, if the specimen is heated, a large compressive stress, perpendicular to the rails, will exist near the specimen corners, positions corresponding to the locations  $x=0$  and  $x=a$  in figure 18.

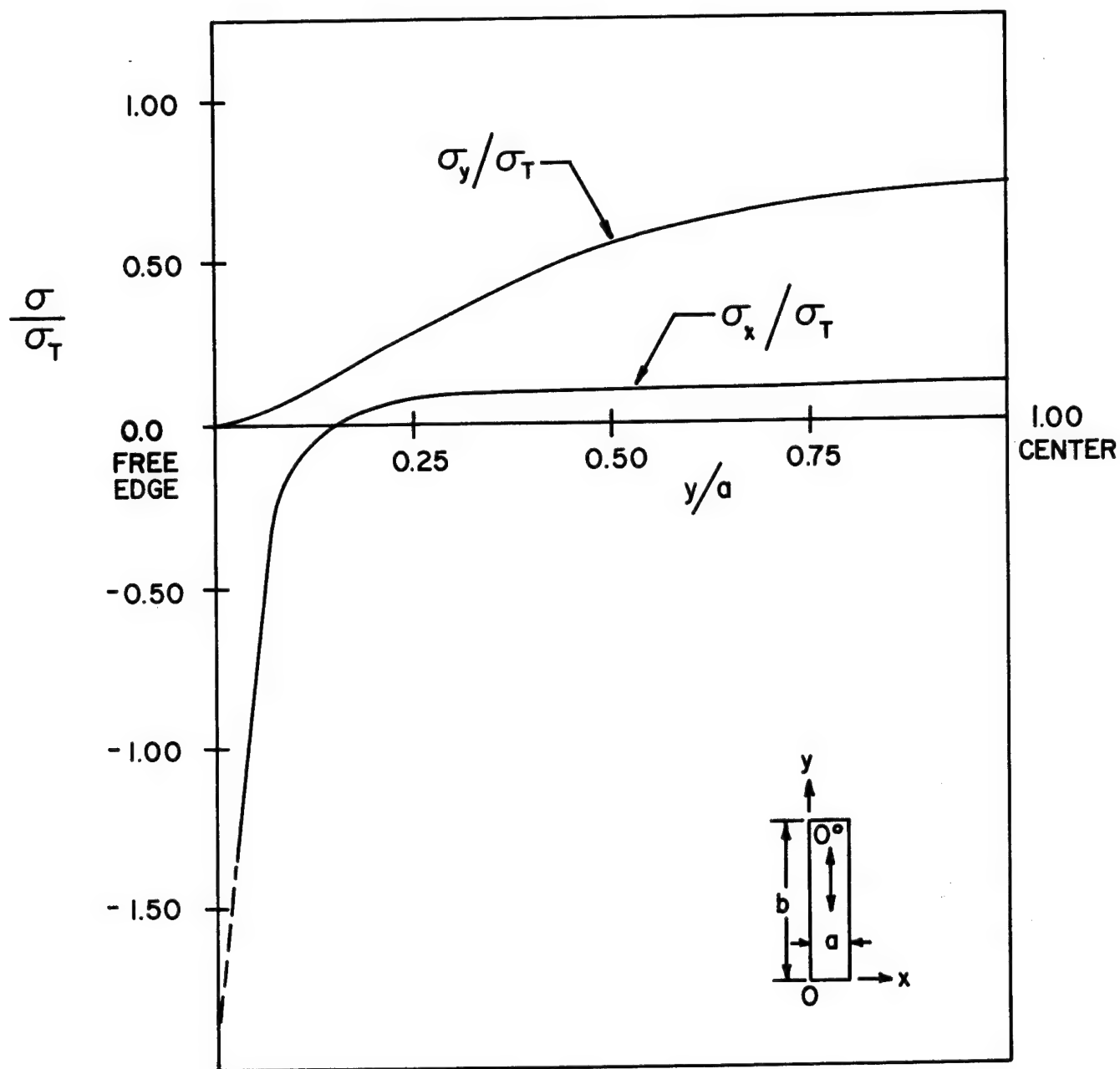


Figure 15 - Nondimensional Normal Stresses  $\sigma_x/\sigma_T$  and  $\sigma_y/\sigma_T$  versus  $y/a$  at  $x=a/2$ .  $[90_{12}]$  Laminate; Specimen Aspect Ratio Equals 2.

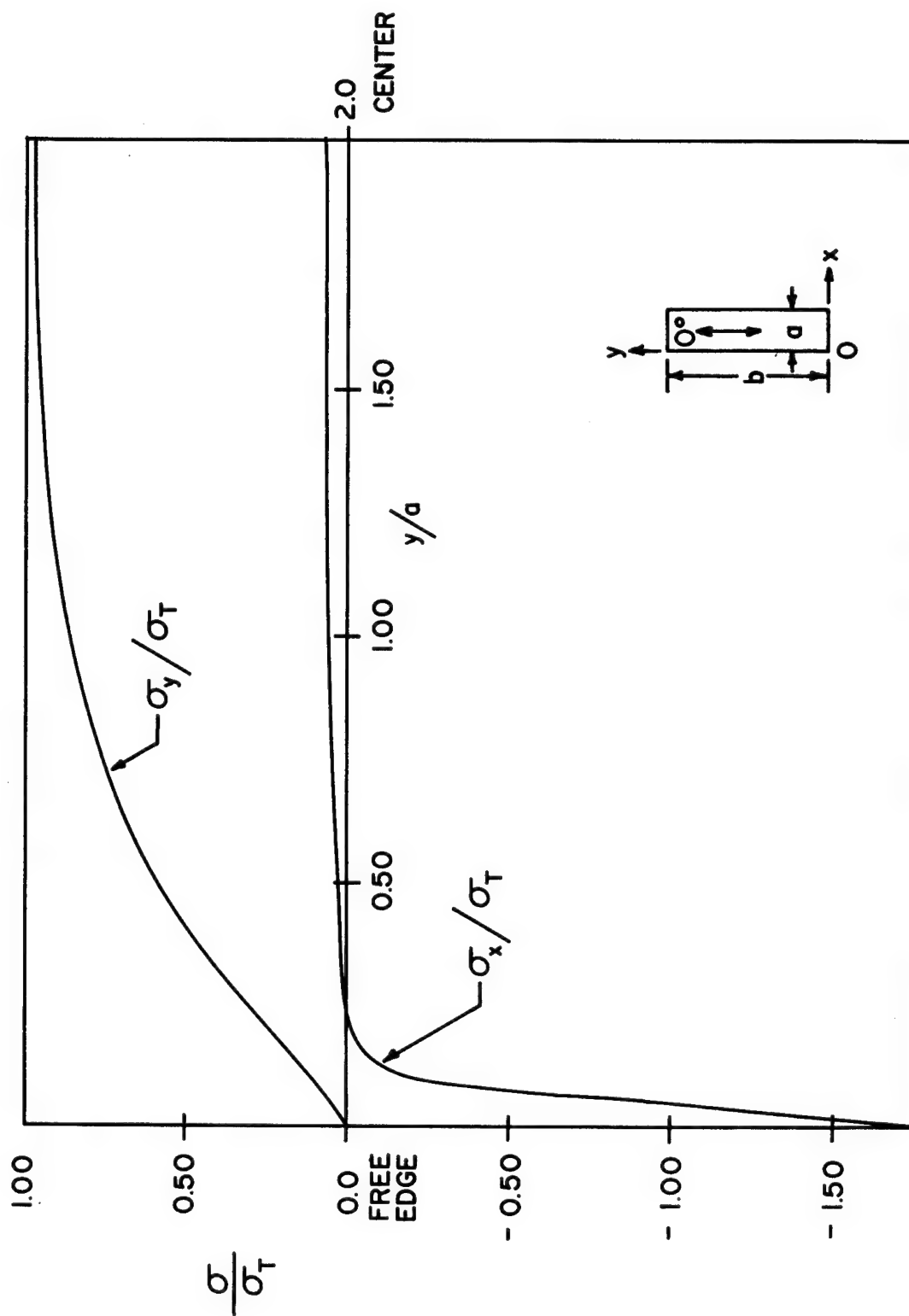


Figure 16 - Nondimensional Normal Stresses  $\sigma_x/\sigma_T$  and  $\sigma_y/\sigma_T$  versus  $y/a$  at  $x=a/2$ .  $[90]_2$  Laminate; Specimen Aspect Ratio Equals 4.



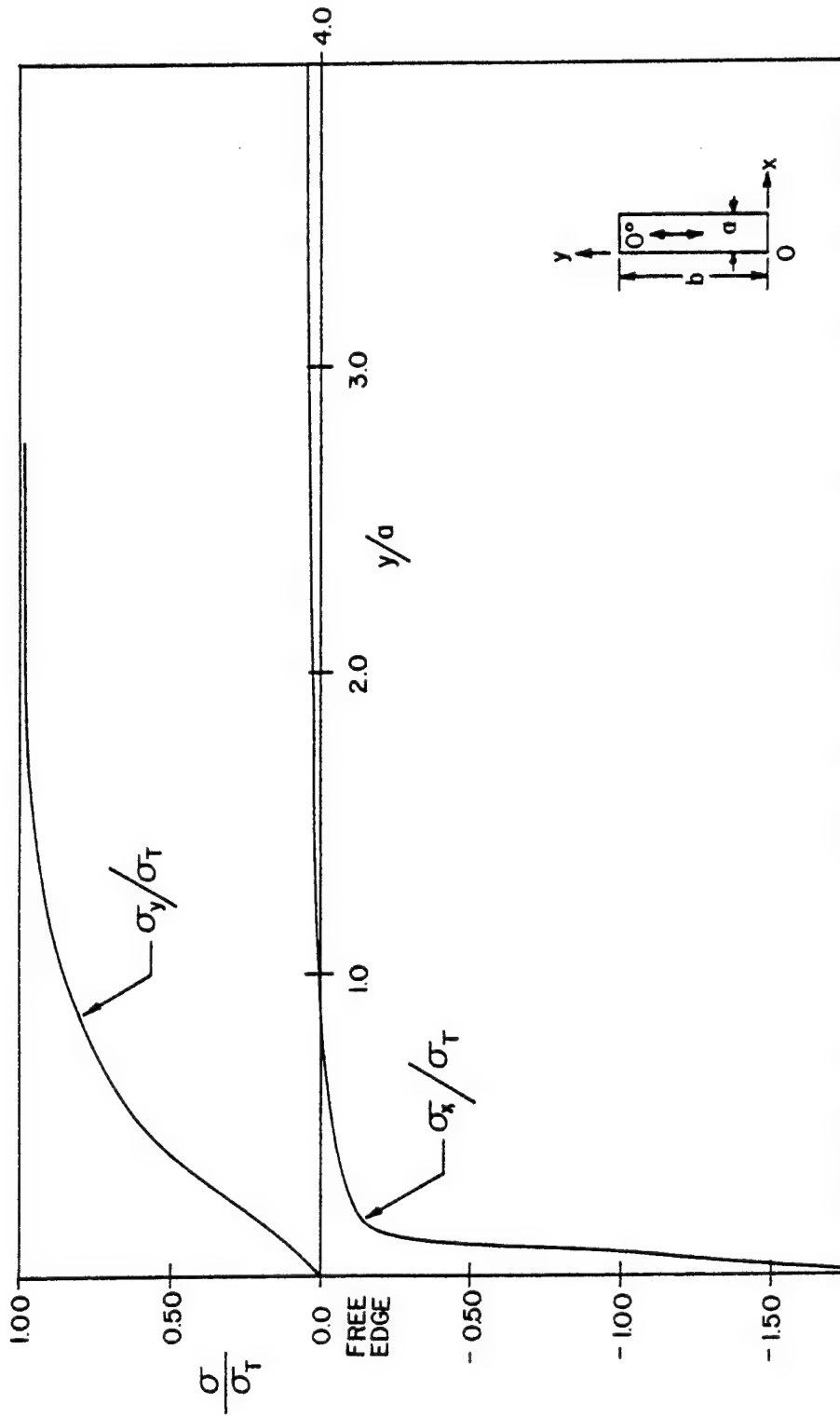


Figure 17 - Nondimensional Normal Stresses  $\sigma_x/\sigma_T$  and  $\sigma_y/\sigma_T$  versus  $y/a$  at  $x=a/2$ .  $[90]_2$  Laminate; Specimen Aspect Ratio Equals 10.

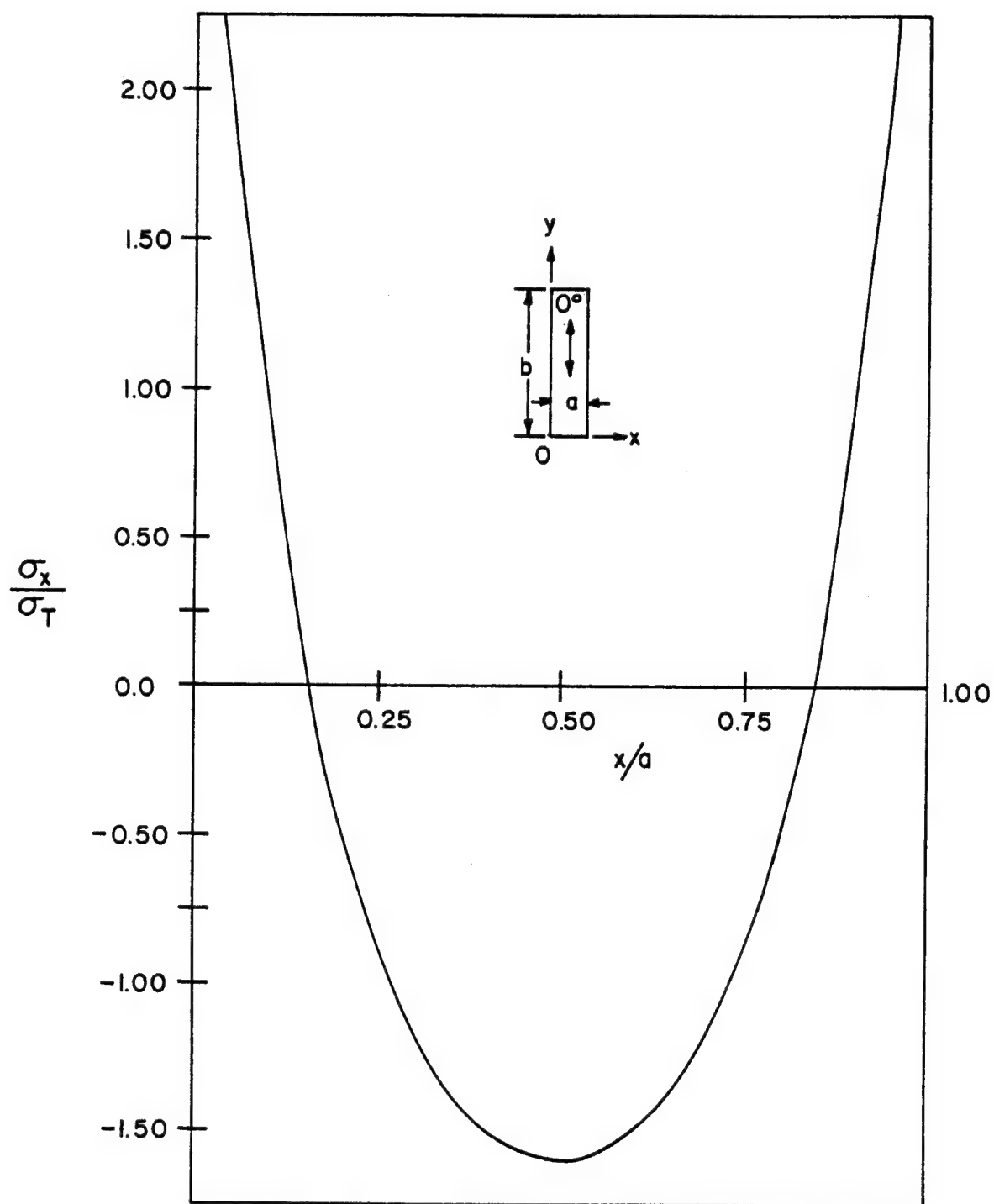


Figure 18 - Nondimensional Normal Stress  $\sigma_x/\sigma_T$  versus  $x/a$  at  $y/a=0.025$ .  
 $[90_{12}]$  Laminate; Specimen Aspect Ratio Equals 10.

To illustrate the nonuniformity of the normal stresses that may exist at the specimen centerline position  $y=b/2$ , figure 19 presents the nondimensionalized stresses  $\sigma_x/\sigma_T$  and  $\sigma_y/\sigma_T$ , as a function of  $x/a$  at  $y=b/2$ , for specimen aspect ratios of 2, 4 and 6. For specimen aspect ratios greater than 6, the normal stresses are constant across the specimen at  $y=b/2$  and cannot be distinguished from those given for an aspect ratio of 6.

#### 4.2.2 Results for the $[0_{12}]$ Laminate

If the specimen fibers are oriented parallel to the rails, the thermal stress problem changes. To illustrate the effect of a uniform  $\Delta T$  on a specimen whose fibers are oriented parallel to the rails, a  $[0_{12}]$  laminate was studied. The coefficient of thermal expansion of the composite specimen in the direction of the rails is nearly zero so that the rail/specimen interface tends to elongate with increases in temperature. This elongation causes tensile stresses in the  $y$ -direction near the center of the specimen. Note that, for this laminate,  $\sigma_T$  will be a positive number if the specimen is heated.

Figure 20 shows the normal stresses that occur along a line at  $x=a/2$  for a  $[0_{12}]$  specimen with aspect ratio of 2. When compared to figure 15, this figure shows that the  $\sigma_x$  stresses in the  $[0_{12}]$  specimen decrease less rapidly with distance away from the free edge. In addition, the  $\sigma_y$  stress distribution shown in figure 20 changes sign, unlike the  $\sigma_y$  distribution shown in figure 15.

When the aspect ratio of the  $[0_{12}]$  specimen is increased, the thermal stress distributions change. Figure 21 shows the distributions

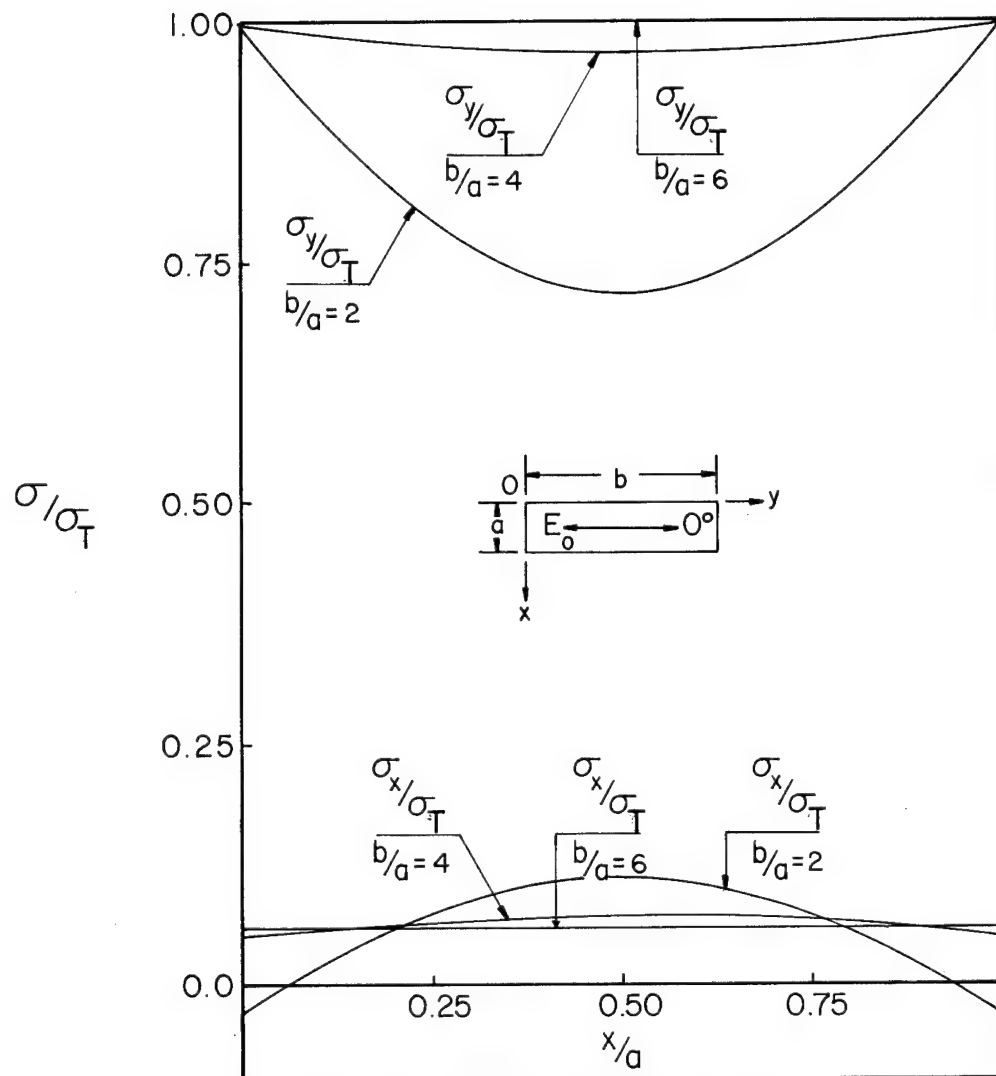


Figure 19 - Nondimensional Normal Stresses  $\sigma_x/\sigma_T$  and  $\sigma_y/\sigma_T$  versus  $x/a$  at  $y=b/2$ .  $[90_{12}]$  Laminate, Aspect Ratios 2, 4 and 6.

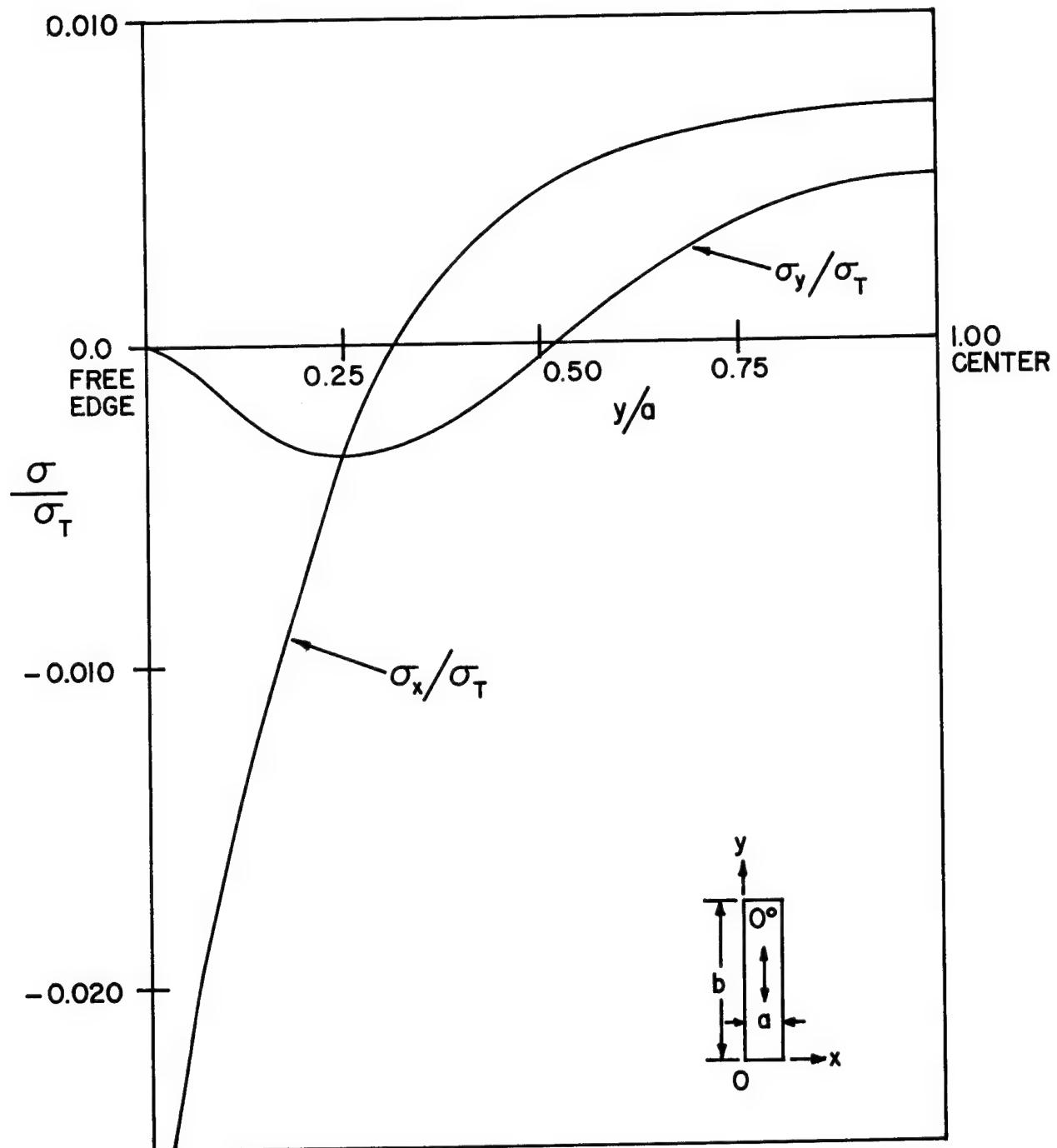


Figure 20 - Nondimensional Normal Stresses  $\sigma_x/\sigma_T$  and  $\sigma_y/\sigma_T$  versus  $y/a$  at  $x=a/2$ .  $[0]_2$  Laminate; Specimen Aspect Ratio Equals 2.

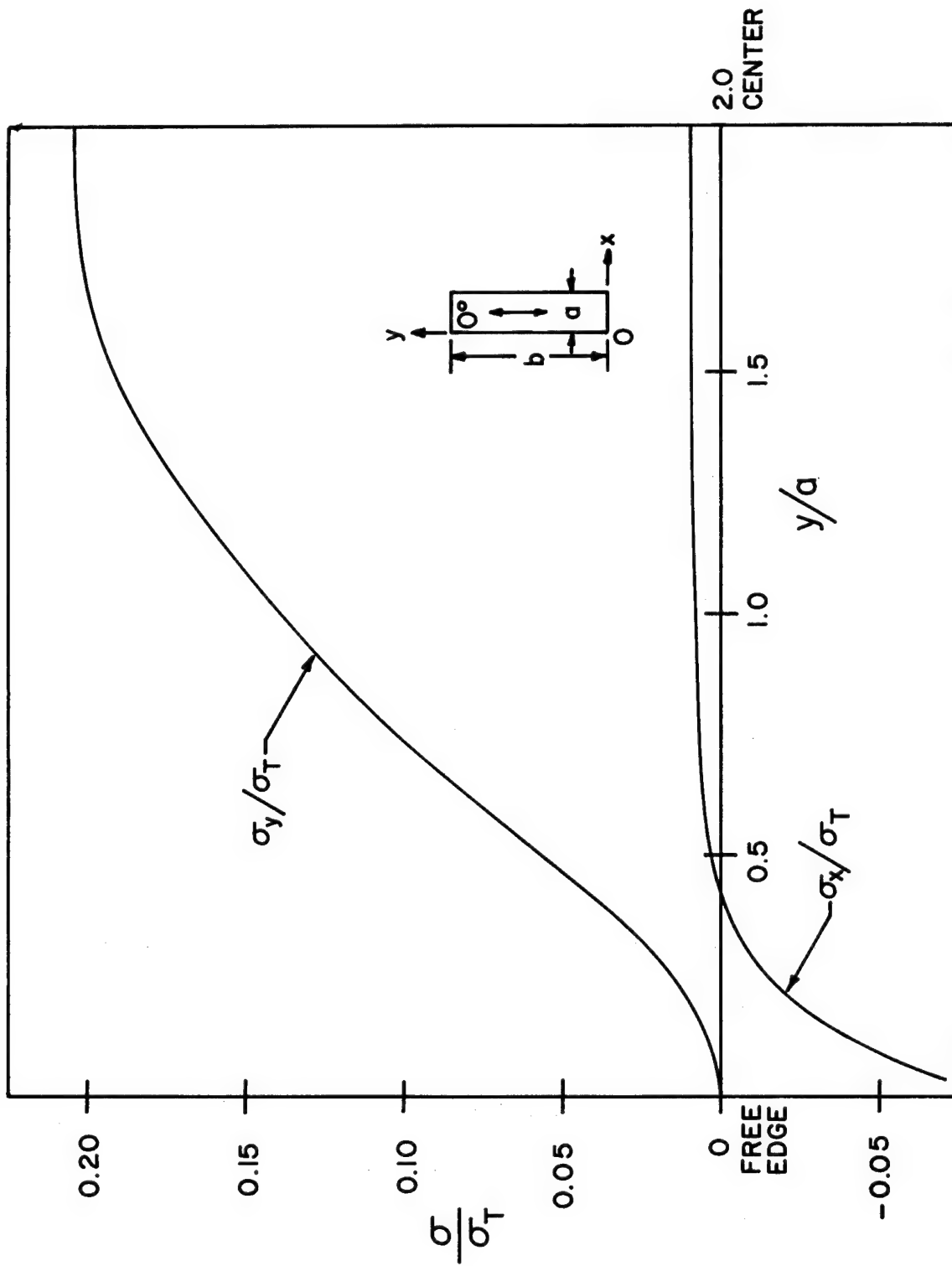


Figure 21 - Nondimensional Normal Stresses  $\sigma_x/\sigma_T$  and  $\sigma_y/\sigma_T$  versus  $y/a$  at  $x=a/2$ .  
 $[0_12]$  Laminate; Specimen Aspect Ratio Equals 4.

of  $\sigma_x$  and  $\sigma_y$  stresses due to a constant  $\Delta T$  for the  $[0]_2$  specimen with an aspect ratio of 4.

Figure 22 shows the distribution of  $\sigma_y/\sigma_T$  at  $x=a/2$  plotted against  $y/a$  for a  $[0]_2$  specimen with an aspect ratio of 10. This figure shows that the  $\sigma_y$  stresses have not yet reached a uniform value at the center region of the plate. This fact is further illustrated in figure 23, where  $\sigma_y/\sigma_T$  is shown plotted against  $x/a$  for a  $[0]_2$  specimen with aspect ratios of 2, 4, 6 and 10. The stress  $\sigma_x$  is not shown in these latter two figures because it is relatively small in comparison to  $\sigma_y$ .

Figure 24 displays the distribution of the normal stress  $\sigma_x$  near the free edge of a  $[0]_2$  specimen with an aspect ratio of 10. This distribution is similar to that seen previously for the  $[90]_2$  laminate. However, since  $\sigma_T$  for the  $[0]_2$  laminate is a positive number for a heated specimen, tensile values of the  $\sigma_x$  stresses will develop near the corners when the  $[0]_2$  specimen is heated. It again should be noted that the value of  $\sigma_T$  used to nondimensionalize the previous results is different for the two laminates. The ratio of  $\sigma_T$  for the  $[0]_2$  laminate to the value of  $\sigma_T$  for the  $[90]_2$  laminate is -9.52. Taking this ratio into account, the values of the  $\sigma_x$  stresses that appear in the corners of both the specimens are of the same order of magnitude, but have different signs. When the specimens are heated, tensile stresses appear near the corners in the  $[0]_2$  laminate while compressive stresses appear in the  $[90]_2$  laminate.

When the  $[0]_2$  laminate is heated, the specimen must resist  $\sigma_x$  tensile stresses, stresses that act in a direction perpendicular to the

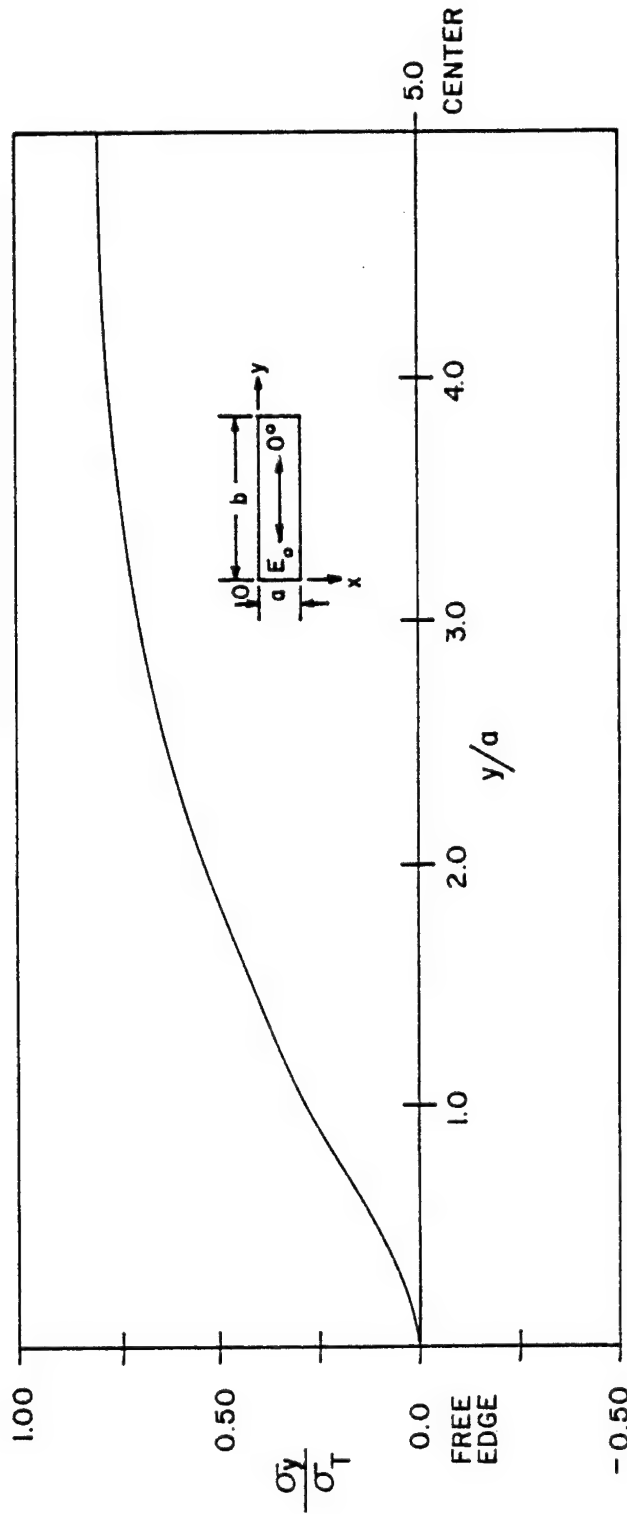


Figure 22 - Nondimensional Stress Distribution  $\sigma_y/\sigma_T$  versus  $y/a$  at  $x=a/2$ .  $[0]_2$  Laminate; Specimen Aspect Ratio Equals 10.



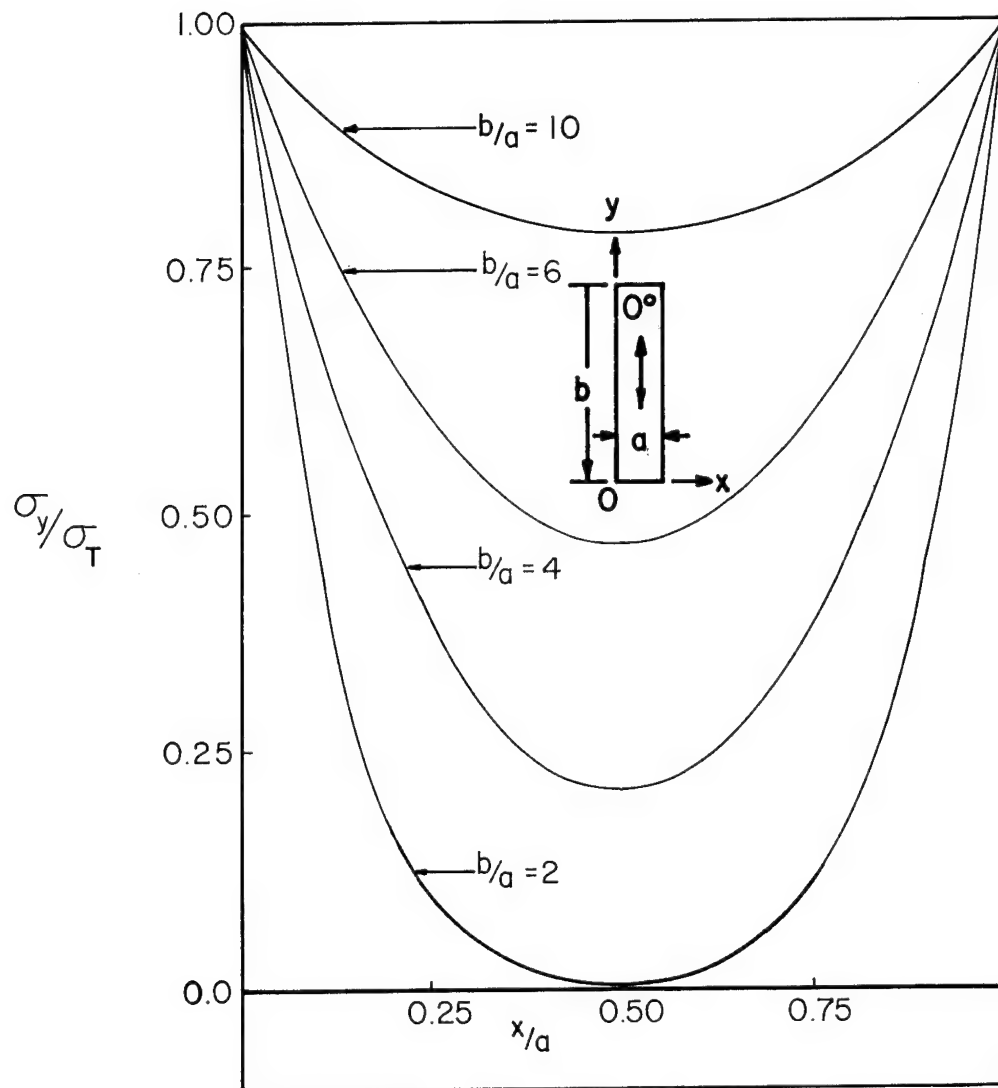


Figure 23 - Nondimensional Normal Stress  $\sigma_y/\sigma_T$  versus  $x/a$  at  $y=b/a$ .  $[0_{12}]$  Laminate, Specimen Aspect Ratios 2, 4, 6, 10.

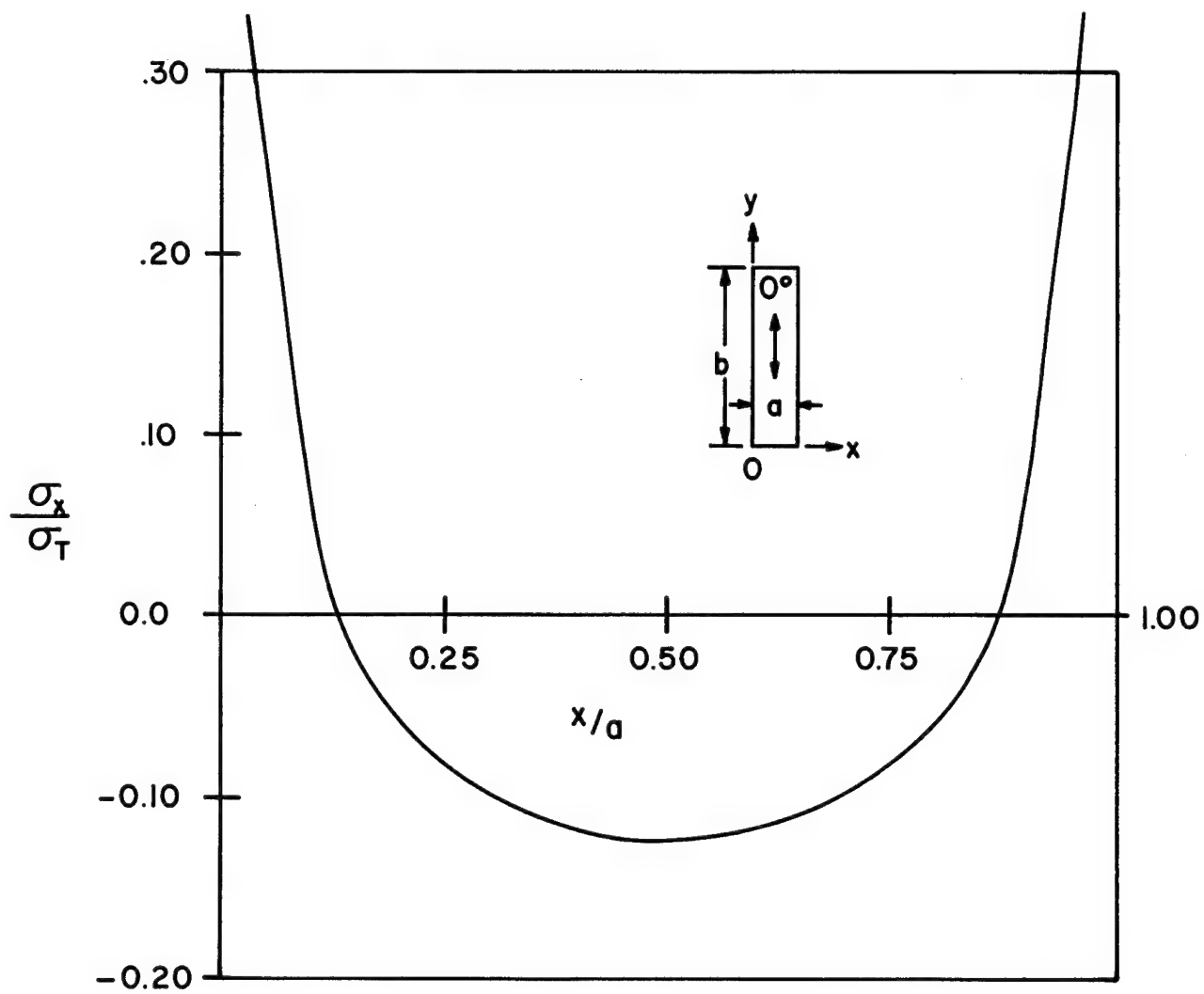


Figure 24 - Normal Stress Distribution  $\sigma_x/\sigma_T$  versus  $x/a$  at  $y/a=0.025$ .  
 $[0_{12}]$  Laminate; Specimen Aspect Ratio Equals 10.

fiber direction; it would appear that the  $[90_{12}]$  specimen is a more satisfactory test configuration than the  $[0_{12}]$  laminate.

Finally, figures 25 and 26 illustrate the typical laminate deflection behavior due to uniform heating for  $[0_{12}]$  and  $[90_{12}]$  specimens with aspect ratios of 4.

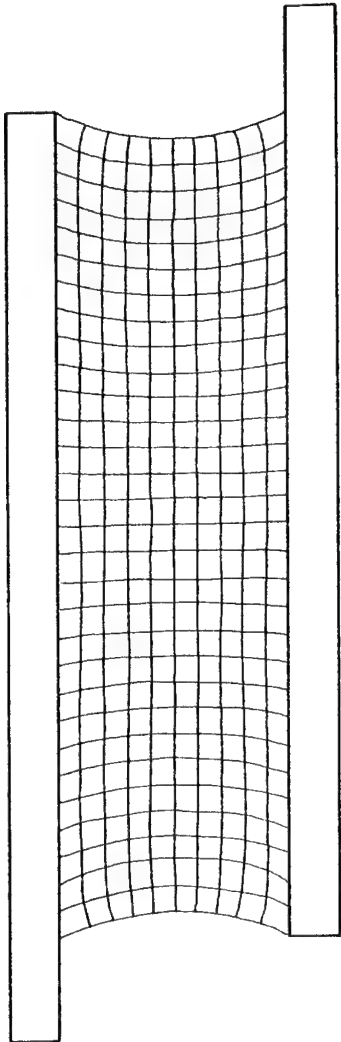


Figure 25 - Specimen Deflection Pattern Caused by Heating to Uniform Temperature.  $[0_{12}]$  Laminate; Specimen Aspect Ratio Equals 4.

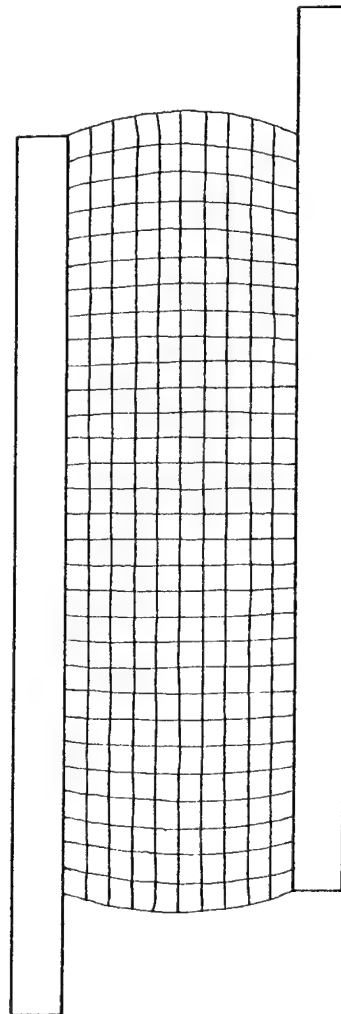


Figure 26 - Specimen Deflection Pattern Caused by Heating to Uniform Temperature.  $[90_{12}]$  Laminate; Specimen Aspect Ratio Equals 4.

## 5.0 CONCLUSIONS

An analytical study has been presented that provides information about the stresses and deflections caused by mechanical loading and thermal expansion of a linear elastic, laminated composite, rail shear test specimen. Results indicate that rail shear testing of the  $[90_{12}]$  graphite/polyimide laminate should provide accurate experimental data for the determination of the shear modulus of the laminate, even for specimen length-to-width ratios as small as 3. Significant experimental error is to be expected for other symmetrical laminates such as the  $[\pm 45_2]_s$ , the  $[90/\pm 45/0]$  laminate or the  $[0_{12}]$  laminate, unless length-to-width ratios larger than 6 are used.

Regions with large shear stresses and normal stresses are found to occur near the corners of the specimens when they are subjected either to mechanical loading or to uniform heating or cooling. This indicates that the rail shear test may not be entirely satisfactory for determining laminate allowable shear stress.

Analysis of the effect of heating an assembled rail shear specimen to a uniform temperature shows that the  $[0_{12}]$  laminate is more adversely affected by differential expansion effects than is the  $[90_{12}]$  laminate. In both cases, regions of large normal stress appear near the corners. However, for large aspect ratio specimens, these stresses are less severe in the case of the  $[90_{12}]$  laminate than they are for the  $[0_{12}]$  laminate.

## APPENDIX

### LAMINA GEOMETRY AND MATERIAL PROPERTIES USED IN THE PRESENT STUDY

#### A. Graphite/Polyimide

$$E_1 = 149.6 \text{ GPa } (21.7 \times 10^6 \text{ psi})$$

$$E_2 = 8.273 \text{ GPa } (1.2 \times 10^6 \text{ psi})$$

$$G_{12} = 4.137 \text{ GPa } (0.6 \times 10^6 \text{ psi})$$

$$\mu_{12} = 0.27$$

$$\mu_{21} = 0.015$$

$$\alpha_1 = 0$$

$$\alpha_2 = 26.1 \times 10^{-6} \text{ m/m/}^\circ\text{C } (14.5 \text{ in./in./}^\circ\text{F})$$

$$a = 7.62 \text{ mm. } (0.30 \text{ inches})$$

$$t = 0.1016 \text{ mm/ply } (0.004 \text{ inches/ply})$$

#### B. Titanium

$$E = 113.8 \text{ GPa } (16.5 \times 10^6 \text{ psi})$$

$$\mu = 0.342$$

$$\alpha = 9 \times 10^{-6} \text{ m/m/}^\circ\text{C } (5 \times 10^{-6} \text{ in./in./}^\circ\text{F})$$

$$\text{Rail width} = 2.54 \text{ cm. } (1 \text{ inch})$$

$$\text{Rail depth} = 2.54 \text{ cm. } (1 \text{ inch})$$

## REFERENCES

1. Purslow, D.: The Shear Properties of Unidirectional Carbon Fibre Reinforced Plastics and their Experimental Determination. C. P. No. 1381, British A.R.C., 1977.
2. Yeow, Y. T.; and Brinson, H. F.: A Comparison of Simple Shear Characterization Methods for Composite Laminates. Composites, Vol. 9, No. 8, 1978, pp. 49 - 55.
3. Bergner, Henry W., Jr.; Davis, John G.; and Herakovich Carl T.: Analysis of Shear Test Methods for Composite Materials. NASA CR-152704, 1977.
4. Coker, E. G.: An Optical Determination of the Variation of Stresses in a Thin Rectangular Plate Subjected to Shear. Proc. Roy. Soc. (London), Series A, vol. 86, 1912, pp. 291 - 319.
5. Whitney, J. M.; Stansbarger, D. L.; and Howell, H. B.: Analysis of Rail Shear Test-Applications and Limitations. J. Comp. Materials, vol. 5, January 1971, pp. 24 - 34.
6. Whitney, James M.: Free Edge Effects in the Measurement of Composite In-Plane Shear Properties. AFML-TR-70-282, U.S. Air Force Materials Laboratory, Air Force Systems Command, Wright-Patterson AFB, Ohio, 1971.
7. Whitney, J. M.: Testing and Characterization of Composite Materials. AFML-TR-71-124, U.S. Air Force Materials Laboratory, Air Force Systems Command, Wright-Patterson AFB, Ohio, 1971.

8. Inglis, C. E.: Stress Distribution in a Rectangular Plate Having Two Opposing Edges Sheared in Opposite Directions. Proc. Roy. Soc. (London), Series A, vol. 102, 1923, pp. 598 - 610.
9. Kuhn, Paul: Stresses in Aircraft and Shell Structures. McGraw-Hill Book Co., Inc., 1956.
10. Hildebrand, F. B.: The Exact Solution of Shear-lag Problems in Flat Panels and Box Beams Assumed Rigid in the Transverse Direction. NACA TN 894, 1943.
11. Goland, M.; and Reissner, E.: The Stresses in Cemented Joints. J. Appl. Mech., vol. 11, 1944, pp. A-17 - A-27.
12. Aleck, B. J.: J. Appl. Mech., vol. 16, 1949, pp. 118 - 122.
13. Kobatake, Yonosuke; and Inoue, Yukihiro: Mechanics of Adhesive Joints, Part I. Residual Stresses. Appl. Sci. Res., Section A, vol. 7, pp. 53 - 64.
14. Whetstone, W. D.: SPAR Structural Analysis System Reference Manual - System Level 11. Volume 1-Program Execution. NASA CR-145098-1, 1977.

1. Report No. NASA CR-3106	2. Government Accession No.	3. Recipient's Catalog No.	
4. Title and Subtitle ANALYSIS OF GRAPHITE/POLYIMIDE RAIL SHEAR SPECIMENS SUBJECTED TO MECHANICAL AND THERMAL LOADING		5. Report Date March 1979	
		6. Performing Organization Code	
7. Author(s) Terry A. Weisshaar and Ramon Garcia		8. Performing Organization Report No. VPI-E-78-27	
		10. Work Unit No.	
9. Performing Organization Name and Address Virginia Polytechnic Institute & State University Aerospace and Ocean Engineering Blacksburg, Virginia 24061		11. Contract or Grant No. NGR-47-004-129	
		13. Type of Report and Period Covered Contractor Report	
12. Sponsoring Agency Name and Address National Aeronautics & Space Administration Washington, DC 20546		14. Sponsoring Agency Code	
15. Supplementary Notes Langley Technical Monitor: Robert R. McWithey Topical Report			
16. Abstract This report discusses the results of a two-dimensional, linear-elastic, finite element analysis of selected graphite/polyimide rail shear test specimens. The study includes the analysis of mechanical loading and the effect of heating the specimen to a uniform temperature. The presence of specimen free edges and their influence on the accuracy of the rail shear test is discussed. Parameters in this analysis include the length-to-width ratio of the specimen and the ply layup for symmetric, balanced laminates. Results presented include shear and normal stress distributions and the deflection behavior of various specimens caused by the mechanical loading and elevated temperature.			
17. Key Words (Suggested by Author(s)) Composites, In-plane Shear, Finite Elements, Rail Shear, Thermal Stresses, Graphite-polyimide		18. Distribution Statement Unclassified - Unlimited Subject Category 24	
19. Security Classif. (of this report) Unclassified	20. Security Classif. (of this page) Unclassified	21. No. of Pages 54	22. Price* \$5.25